Electronic supporting information for

"Experimental evidence for CH···π interaction-mediated atabilization of the square form in phenylglycine-incorporated ascidiacyclamide"

Akiko Asano*, Katsuhiko Minoura, Takeshi Yamada, and Mitsunobu Doi

Faculty of Pharmacy, Osaka Medical and Pharmaceutical University, 4-20-1 Nasahara, Takatsuki, Osaka 569-1094, Japan.

Contents:

Synthesis and characterization of the peptides Xb and Xc (X=2-4).

General Experimental Methods

Pure products were obtained after liquid chromatography using Merck silica gel 60 (40-63 μm). Analytical thin-layer chromatography was carried out on Merck silica gel F_{254} plates with the following solvent system (v/v); chloroform : methanol : acetic acid (95 : 10 : 3). The plates were visualized with UV light (λ = 254 nm) and revealed with a 5 % solution of ninhydrin in ethanol. ^{1}H NMR spectra were recorded on an Agilent DD2 600-MHz NMR spectrometer (Agilent Technologies, California, USA). Peptide concentrations were about 5.0 mM in CD_3CN. Chemical shifts were measured relative to internal trimethylsilane at 0.00 ppm. The protons were assigned using two dimensional correlated spectroscopy (2D-COSY) and rotating-frame Overhauser effect spectroscopy (ROESY; mixing time = 500 ms). Low-resolution mass spectra (LR-MS) were obtained by using matrix-assisted laser desorption ionization (MALDI-TOF) mass spectroscopy on a Bruker microflex LRF (Bruker, Massachusetts, USA).

Synthesis of Boc-D-Val(Thz)-OMe

Boc-D-Val(Thz)-OMe was prepared according to previous report (Y. Hamada *et. al*., *J. Org. Chem*., 1987, **52**, 1252-1255) (Scheme S1). N-(*tert*-butoxycarbonyl)-D-valine (Boc-D-Val-OH) was first converted to the corresponding methyl ester by using methyl iodide in the presence of potassium hydrogen carbonate in N, N-dimethylformamide (DMF) at room temperature. The methyl ester was reduced with lithium chloride-sodium borohydride in tetrahydrofuran (THF) to give the amino alcohol derivative. Oxidation of the amino alcohol derivative was conveniently accomplished by the dimethyl sulfoxide (DMSO) oxidation using sulfur trioxide-pyridine complex ($Py{\cdot}SO_3$) in the presence of trimethylamine (Et_3N), giving the amino aldehyde derivative. Condensation of the amino aldehyde derivative with L-cysteine methyl ester (H-L-Cys-OMe) afforded the thiazolidine derivative as a mixture of C-2 epimers. Oxidation of the thiazolidine derivative to the Boc-D-Val(Thz)-OMe was performed with activated manganese dioxide (Sigma-Aldrich Co. Llc., St. Louis, USA) in benzene.

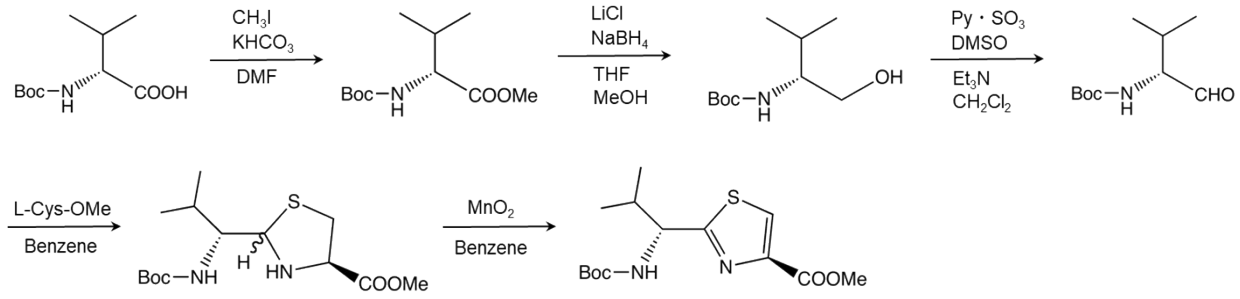

Scheme S1

General procedure for the condensation

Peptides were synthesized by a conventional liquid-phase method according to Scheme S2. The liner peptide were synthesized using 1-hydroxy-benzotiazole (HOBt) (Watanabe Chemical Ind. Ltd., Hiroshima, Japan) and 1-ethyl-3-(3-dimethylaminopropyl)carbodiimide hydrochloride (EDC·HCl) (Watanabe Chemical Ind. Ltd., Hiroshima, Japan), and cyclization was conducted with benzotriazolyloxy-tris(pyrrolidino)-phosphonium hexafluorophosphate (PyBOP) (Watanabe Chemical Ind. Ltd., Hiroshima, Japan) in the presence of 4-dimethylaminopyridine (DMAP) (Nacalai tesque, Kyoto, Japan).

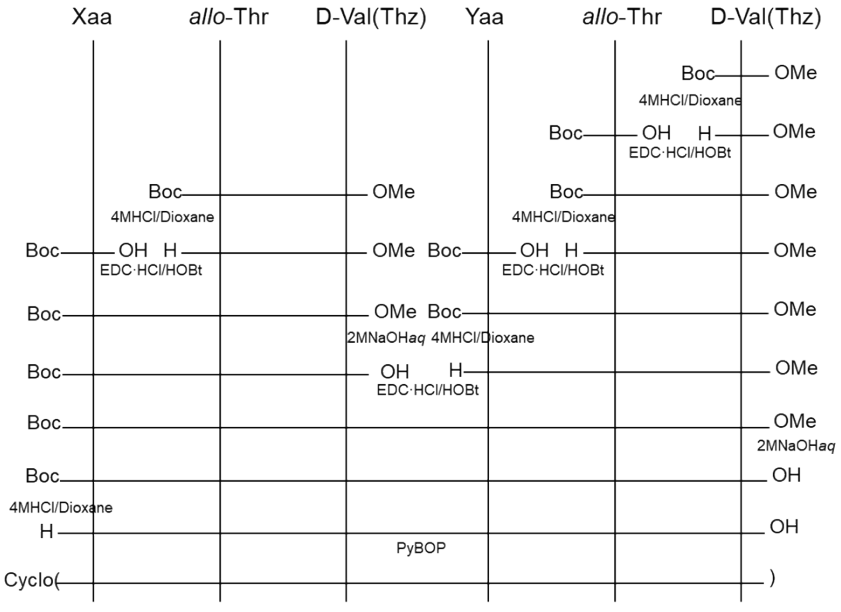

Xb; (Xaa,Yaa) = **2b**; (Val,Chg), **3b**; (Abu,Chg), **4b**; (Ala,Chg)

Xc; (Xaa,Yaa) = **2c**; (Val,Phg), **3c**; (Abu,Phg), **4c**; (Ala,Phg)

Scheme S2

Synthesis of oxazoline rings

The oxazoline (Oxz) rings were formed by reacting the Ile–*allo*-Thr moiety with bis(2-methoxyethyl)aminosulfur trifluoride (Deoxo-Fluor) (Fujifilm Wako Pure Chemical, Osaka, Japan) according to previous report (A. J. Phillips *et. al*., *Org. Lett*., 2000, **2**, 1165-1168) (Scheme S3).

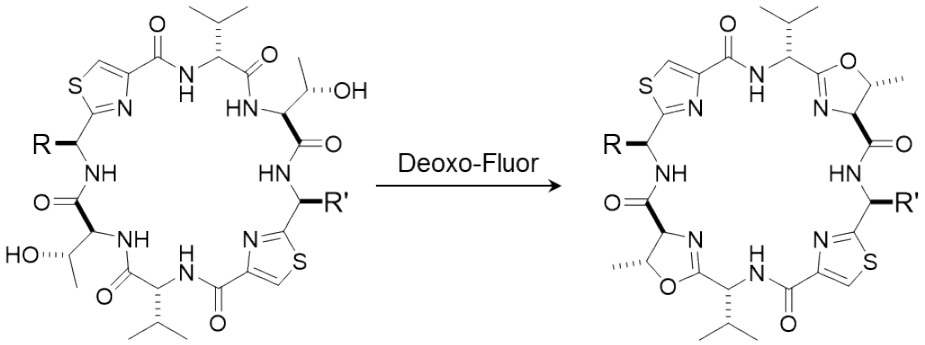

2b: R = $CH(CH_3)_2$, R' = cyclohexane
3b: R = CH_2CH_3, R' = cyclohexane
4b: R = CH_3, R' = cyclohexane
2c: R = $CH(CH_3)_2$, R' = benzene
3c: R = CH_2CH_3, R' = benzene
4c: R = CH_3, R' = benzene

Scheme S3

Characterization of peptide 2b

MALDI-TOF MS calcd for $[C_{37}H_{52}N_8O_6S_2 + H]^+$ = 769.36, found *m*/*z* 769.41. ^{1}H NMR (600 MHz, CD_3CN, 298 K) δ = 7.89 (d, 1H, NH Val^1, J = 6.6 Hz); 7.82 (d, 1H, NH Chg^5, J = 7.2 Hz); 7.76 (s, 1H, H Thz^{4or8}); 7.75 (s, 1H, H Thz^{4or8}); 7.21 (d, 1H, NH D-Val^{3or7}, J = 9.6 Hz); 7.20 (d, 1H, NH D-Val^{3or7}, J = 10.2 Hz); 5.15 (dd, 1H, $^{\alpha}$H D-Val^{3or7}, J = 10.2, 5.4 Hz); 5.14 (dd, 1H, $^{\alpha}$H D-Val^{3or7}, J = 10.2, 6.0 Hz); 4.83 (qd, 1H, $^{\beta}$H Oxz^{2or6}, J = 4.8, 6.6 Hz); 4.82 (qd, 1H, $^{\beta}$H Oxz^{2or6}, J = 4.8, 6.6 Hz); 4.60 (t, 1H, $^{\alpha}$H Chg^5, J = 7.2 Hz); 4.54 (t, 1H, $^{\alpha}$H Val^1, J = 6.6 Hz); 4.29 (dd., 1Hx2, $^{\alpha}$H Oxz^{2,6}, J = 4.8, 1.2 Hz); 2.32 (m, 1Hx2, $^{\beta}$H D-Val^{3,7}); 2.18 (oct., 1H, $^{\beta}$H Val^1, J = 6.6 Hz); 1.87 (m, 1H, $^{\beta}$H Chg^5); 1.68-0.89 (m, 10H, cyclohexyl CH_2 Chg^5); 1.43 (d, 3H, $^{\gamma}$H Oxz^{2or6}, J = 6.6 Hz); 1.41 (d, 3H, $^{\gamma}$H Oxz^{2or6}, J = 6.6 Hz); 1.10 (d, 3Hx2, $^{\gamma 1}$H D-Val^{3,7}, J = 6.6 Hz); 1.03 (d, 3Hx2, $^{\gamma 2}$H D-Val^{3,7}, J = 6.6 Hz); 0.84 (d, 3Hx2, $^{\gamma}$H Val^1, J = 6.6 Hz).

Characterization of peptide 3b

MALDI-TOF MS calcd for $[C_{36}H_{50}N_8O_6S_2 + H]^+$ = 755.34, found *m*/*z* 755.37. ^{1}H NMR (600 MHz, CD_3CN, 298 K) δ = 7.88 (d, 1H, NH Abu^1, J = 6.6 Hz); 7.77 (d, 1H, NH Chg^5, J = 7.8 Hz); 7.72 (s, 1H, H Thz^{4or8}); 7.71 (s, 1H, H Thz^{4or8}); 7.21 (d, 1H, NH D-Val^3, J = 10.2 Hz); 7.16 (d, 1H, NH D-Val^7, J = 10.2 Hz); 5.16 (dd, 1H, $^{\alpha}$H D-Val^3, J = 10.2, 6.6 Hz); 5.13 (dd, 1H, $^{\alpha}$H D-Val^7, J = 10.2, 6.6 Hz); 4.84 (qd, 1H, $^{\beta}$H Oxz^6, J = 6.0, 4.8 Hz); 4.81 (qd, 1H, $^{\beta}$H Oxz^2, J = 6.6, 4.2 Hz); 4.74 (q, 1H, $^{\alpha}$H Abu^1, J = 6.6 Hz); 4.61 (t, 1H, $^{\alpha}$H Chg^5, J = 7.8 Hz); 4.30 (d, 1H, $^{\alpha}$H Oxz^2, J = 4.2 Hz); 4.28 (d, 1H, $^{\alpha}$H Oxz^6, J = 4.8 Hz); 2.33 (oct., 1Hx2, $^{\beta}$H D-Val^{3,7}, J = 6.6 Hz); 1.95 (m, 1H, $^{\beta 12}$H Abu^1); 1.82 (m, 1H, $^{\beta 13}$H Abu^1); 1.89 (m, 1H, $^{\beta}$H Chg^5); 1.68-0.94 (m, 10H, cyclohexyl CH_2, Chg^5); 1.43 (d, 3H, $^{\gamma}$H Oxz^2, J = 6.6 Hz); 1.40 (d, 3H, $^{\gamma}$H Oxz^6, J = 6.0 Hz); 1.12 (d, 3H, $^{\gamma 1}$H D-Val^3, J = 6.6 Hz); 1.11(d, 3H, $^{\gamma 1}$H D-Val^7, J = 6.6 Hz); 1.04 (d, 3Hx2, $^{\gamma 2}$H D-Val^{3,7}, J = 6.6 Hz); 0.73 (t, 3H, $^{\gamma}$H Abu^1, J = 7.8 Hz).

Characterization of peptide 4b

MALDI-TOF MS calcd for $[C_{35}H_{50}N_8O_6S_2 + H]^+$ = 741.32, found *m*/*z* 741.21. ^{1}H NMR (600 MHz, CD_3CN, 298 K) δ = 7.80 (d, 1H, NH Ala^1, J = 6.6 Hz); 7.67 (d, 1H, NH Chg^5, J = 8.4 Hz); 7.63 (s, 1Hx2, H Thz^{4,8}); 7.22 (d, 1H, NH D-Val^3, J = 10.5 Hz); 7.13 (d, 1H, NH D-Val^7, J = 10.5 Hz); 5.17 (dd, 1H, $^{\alpha}$H D-Val^3, J = 10.5, 4.2 Hz); 5.13 (dd, 1H, $^{\alpha}$H D-Val^7, J = 10.5, 5.4 Hz); 4.87 (qd, 1H, $^{\beta}$H Oxz^6, J = 6.6, 4.2 Hz); 4.83 (quint., 1H, $^{\alpha}$H Ala^1, J = 6.6 Hz); 4.79 (qd, 1H, $^{\beta}$H Oxz^2, J = 6.0, 4.2 Hz); 4.61 (t, 1H, $^{\alpha}$H Chg^5, J = 8.4 Hz); 4.30 (dd, 1H, $^{\alpha}$H Oxz^2, J = 4.2, 0.6 Hz); 4.29 (dd, 1H, $^{\alpha}$H Oxz^6, J = 4.2, 0.6 Hz); 2.34 (m, 1Hx2, $^{\beta}$H D-Val^{3,7}); 1.94 (m, 1H, $^{\beta}$H Chg^5); 1.71-1.03 (m, 10H, cyclohexyl CH_2, Chg^5); 1.44 (d, 3H, $^{\beta}$H Ala^1, J = 6.6 Hz); 1.43 (d, 3H, $^{\gamma}$H Oxz^2, J = 6.0 Hz); 1.40 (d, 3H, $^{\gamma}$H Oxz^6, J = 6.6 Hz); 1.11 (d, 3H, $^{\gamma 1}$H D-Val^3, J = 6.6 Hz); 1.10 (d, 3H, $^{\gamma 1}$H D-Val^7, J = 6.6 Hz); 1.06 (d, 3Hx2, $^{\gamma 2}$H D-Val^{3,7}, J = 6.6 Hz).

Characterization of peptide 2c

MALDI-TOF MS calcd for $[C_{37}H_{46}N_8O_6S_2 + H]^+$ = 763.31, found *m*/*z* 763.37. ^{1}H NMR (600 MHz, CD_3CN, 298 K) δ = 8.58 (d, 1H, NH Phg^5, J = 7.8 Hz); 8.09 (s, 1H, H Thz^{4or8}); 8.05 (d, 1H, NH Val^1, J = 8.4 Hz); 7.94 (s, 1H, H Thz^{4or8}); 7.55 (d, 1H, NH D-Val^7, J = 10.2 Hz); 7.26 (d, 1H, NH D-Val^3, J = 10.2 Hz); 7.21-7.17 (m, 3H, ArH Phg^5); 7.06-7.04 (m, 2H, ArH Phg^5); 5.76 (dd, $^{\alpha}$H Phg^5, J = 7.8, 1.8 Hz); 5.20 (dd, 1H, $^{\alpha}$H D-Val^7, J = 10.0, 6.6 Hz); 5.09 (dd, 1H, $^{\alpha}$H D-Val^3, J = 10.2, 8.4 Hz); 4.72 (quint., 1H, $^{\beta}$H Oxz^2, J = 6.0 Hz); 4.69 (quint., 1H, $^{\beta}$H Oxz^6, J = 6.0 Hz); 4.62 (ddd, 1H, $^{\alpha}$H Val^1, J = 8.4, 3.6, 1.8 Hz); 4.40 (dd, 1H, $^{\alpha}$H Oxz^6, J = 6.0, 1.8 Hz); 4.24 (dd, 1H, $^{\alpha}$H Oxz^2, J = 6.0, 1.8 Hz); 2.36 (m, 1H, $^{\beta}$H D-Val^3); 2.31 (oct., 1H, $^{\beta}$H D-Val^7, J = 6.6 Hz); 1.78 (sept.d, 1H, $^{\beta}$H Val^1, J = 6.6, 3.6 Hz); 1.43 (d, 3H, $^{\gamma}$H Oxz^6, J = 6.0 Hz); 1.31 (d, 3H, $^{\gamma}$H Oxz^2, J = 6.0 Hz); 1.15 (d, 3H, $^{\gamma 1}$H D-Val^7, J = 6.6 Hz); 1.13 (d, 3H, $^{\gamma 1}$H D-Val^3, J = 6.0 Hz); 0.99 (d, 3H, $^{\gamma 2}$H D-Val^7, J = 6.6 Hz); 0.96 (d, 3H, $^{\gamma 2}$H D-Val^3, J = 6.0 Hz); 0.32 (d, 3H, $^{\gamma 1}$H Val^1, J = 6.6 Hz); 0.29 (d, 3H, $^{\gamma 1}$H Val^1, J = 6.6 Hz).

Characterization of peptide 3c

MALDI-TOF MS calcd for $[C_{36}H_{44}N_8O_6S_2 + H]^+$ = 749.29, found *m*/*z* 749.36. ^{1}H NMR (600 MHz, CD_3CN, 298 K) δ = 8.50 (d, 1H, NH Phg^5, J = 7.8 Hz); 8.09 (d, 1H, NH Abu^1, J = 7.8 Hz); 8.06 (s, 1H, H Thz^{4or8}); 7.91 (s, 1H, H Thz^{4or8}); 7.50 (d, 1H, NH D-Val^7, J = 9.6 Hz); 7.25 (d, 1H, NH D-Val^3, J = 10.2 Hz); 7.22-7.17 (m, 3H, ArH Phg^5); 7.10-7.07 (m, 2H, ArH Phg^5); 5.79 (dd, 1H, $^{\alpha}$H Phg^5, J = 7.8, 1.8 Hz); 5.16 (dd, 1H, $^{\alpha}$H D-Val^7, J = 9.6, 7.8 Hz); 5.09 (dd, 1H, $^{\alpha}$H D-Val^3, J = 10.2, 8.4 Hz); 4.75 (m, 1H, $^{\alpha}$H Abu^1); 4.70 (quint., 1H, $^{\beta}$H Oxz^6, J = 6.0 Hz); 4.68 (quint., 1H, $^{\beta}$H Oxz^2, J = 6.0 Hz); 4.39 (dd, 1H, $^{\alpha}$H Oxz^6, J = 6.0, 1.8 Hz); 4.25 (dd, 1H, $^{\alpha}$H Oxz^2, J = 6.0, 1.2 Hz); 2.36 (m, 1Hx2, $^{\beta}$H D-Val^{3,7}); 1.43 (d, 3H, $^{\gamma}$H Oxz^6, J = 6.0 Hz); 1.41 (m, 1H, Abu^1); 1.29 (d, 3H, $^{\gamma}$H Oxz^2, J = 6.0 Hz); 1.16 (d, 3H, $^{\gamma 1}$H D-Val^7, J = 6.6 Hz); 1.14 (d, 3H, $^{\gamma 1}$H D-Val^3, J = 6.6 Hz); 1.00 (d, 3H, $^{\gamma 2}$H D-Val^7, J = 6.6 Hz); 0.97 (d, 3H, $^{\gamma 2}$H D-Val^3, J = 6.6 Hz); -0.02 (t, 3H, $^{\gamma}$H Abu^1, J = 7.2 Hz).

Characterization of peptide 4c

MALDI-TOF MS calcd for $[C_{35}H_{42}N_8O_6S_2 + H]^+$ = 735.28, found *m*/*z* 735.36. ^{1}H NMR (600 MHz, CD_3CN, 298 K) δ = 8.44 (d, 1H, NH Phg^5, J = 8.4 Hz); 7.99 (d, 1H, NH Ala^1, J = 6.6 Hz); 7.99 (s, 1H, H Thz^{4or8}); 7.92 (s, 1H, H Thz^{4or8}); 7.54 (d, 1H, NH D-Val^7, J = 10.2 Hz); 7.29 (d, 1H, NH D-Val^3, J = 9.6 Hz); 7.26-7.23 (m, 3H, ArH Phg^5); 7.17-7.14 (m, 2H, ArH Phg^5); 5.91 (dd, 1H, $^{\alpha}$H Phg^5, J = 8.4, 1.2 Hz); 5.19 (dd, 1H, $^{\alpha}$H D-Val^7, J = 10.2, 6.6 Hz); 5.10 (dd, 1H, $^{\alpha}$H D-Val^3, J = 9.6, 6.6 Hz); 4.74 (quint., 1H, $^{\beta}$H Oxz^6, J = 6.0 Hz); 4.72 (quint.d, 1H, $^{\alpha}$H Ala^1, J = 6.6, 1.2 Hz); 4.60 (quint., 1H, $^{\beta}$H Oxz^2, J = 6.0 Hz); 4.39 (dd, 1H, $^{\alpha}$H Oxz^6, J = 6.0, 1.2 Hz); 4.20 (dd, 1H, $^{\alpha}$H Oxz^2, J = 6.0, 1.2 Hz); 2.31 (oct., 1Hx2, $^{\beta}$H D-Val^{3,7}, J = 6.6 Hz); 1.45 (d, 3H, $^{\gamma}$H Oxz^6, J = 6.0 Hz); 1.21 (d, 3H, $^{\gamma}$H Oxz^2, J = 6.0 Hz); 1.13 (d, 3H, $^{\gamma 1}$H D-Val^7, J = 6.6 Hz); 1.11 (d, 3H, $^{\gamma 1}$H D-Val^3, J = 6.6 Hz); 1.01 (d, 3H, $^{\gamma 2}$H D-Val^7, J = 6.6 Hz); 0.98 (d, 3H, $^{\gamma 2}$H D-Val^3, J = 6.6 Hz); 0.86 (d, 3H, $^{\beta}$H Ala^1, J = 6.6 Hz).

^{1}H NMR spectra of peptides 2b

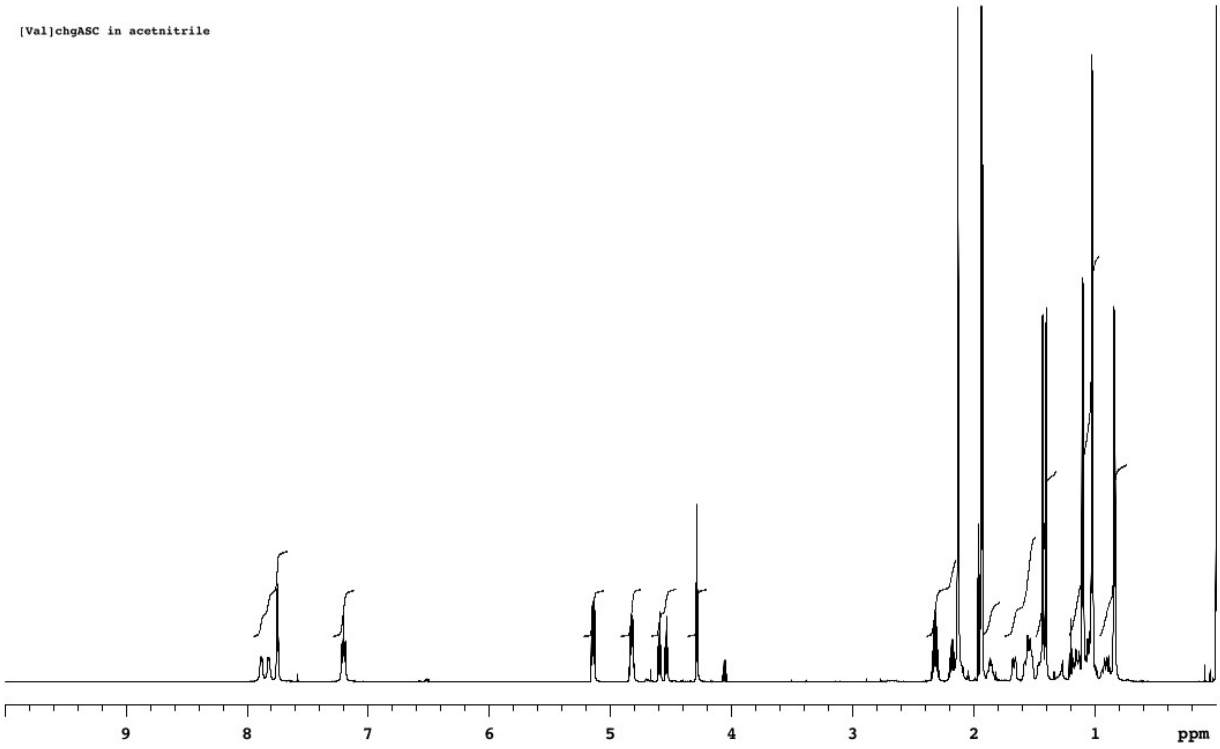

Fig. S1 1D ^{1}H NMR spectrum of peptide **2b** in CD_3CN at 298 K.

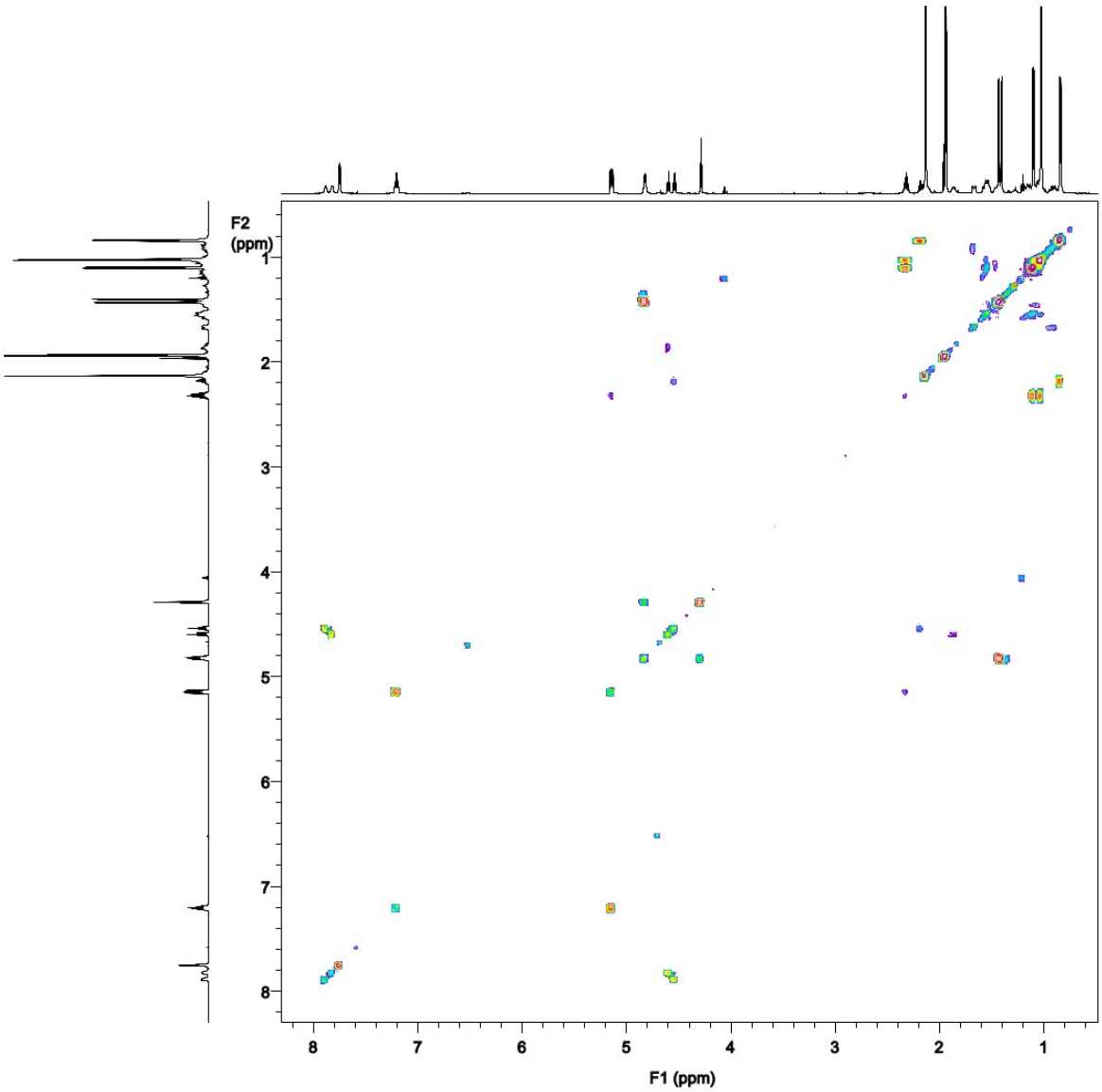

Fig. S2 2D ^{1}H-^{1}H COSY spectrum of peptide **2b** in CD_3CN at 298 K.

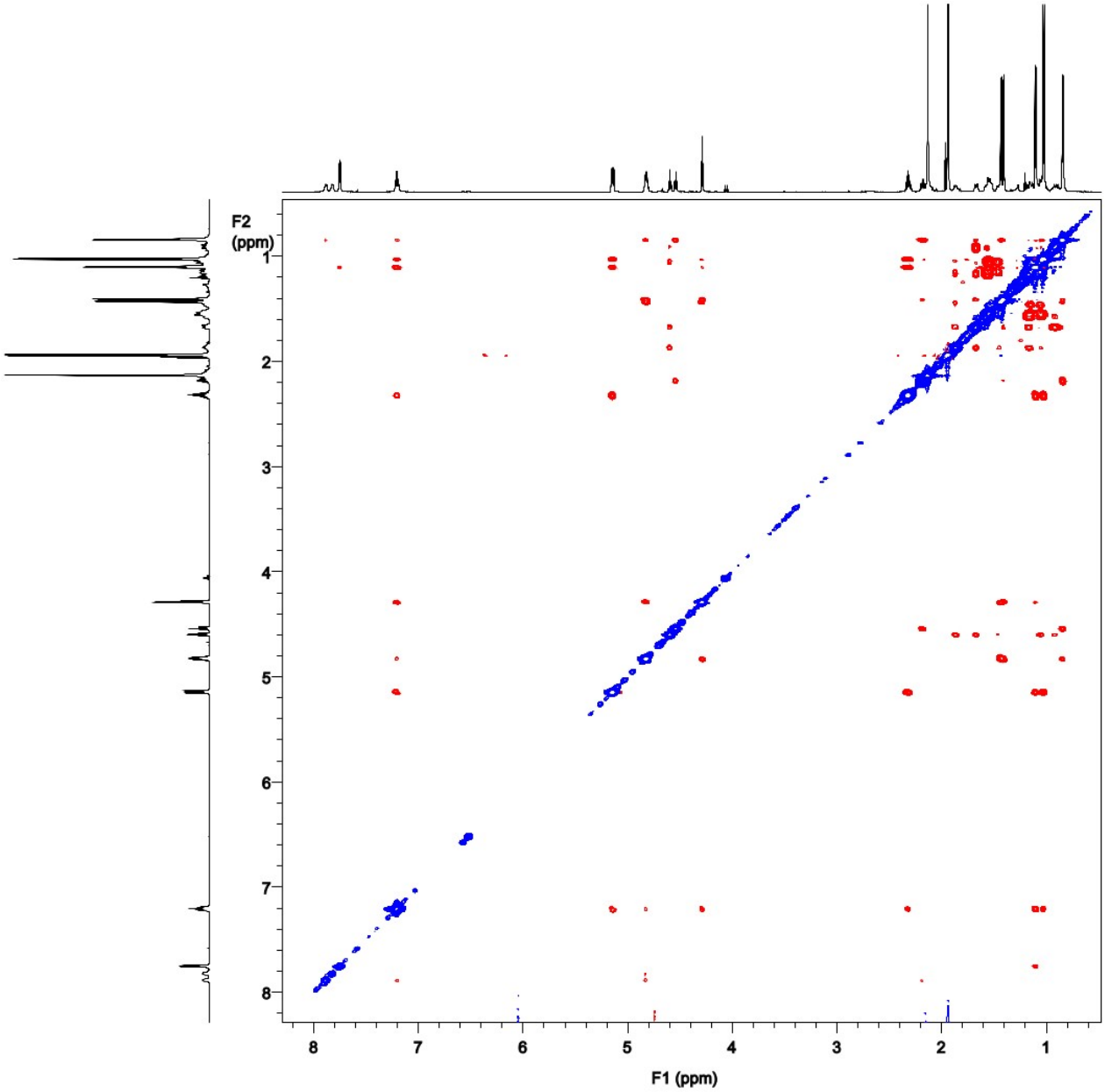

Fig. S3 2D ^{1}H-^{1}H ROESY spectrum of peptide **2b** in CD_3CN at 298 K.

^{1}H NMR spectra of peptides 3b

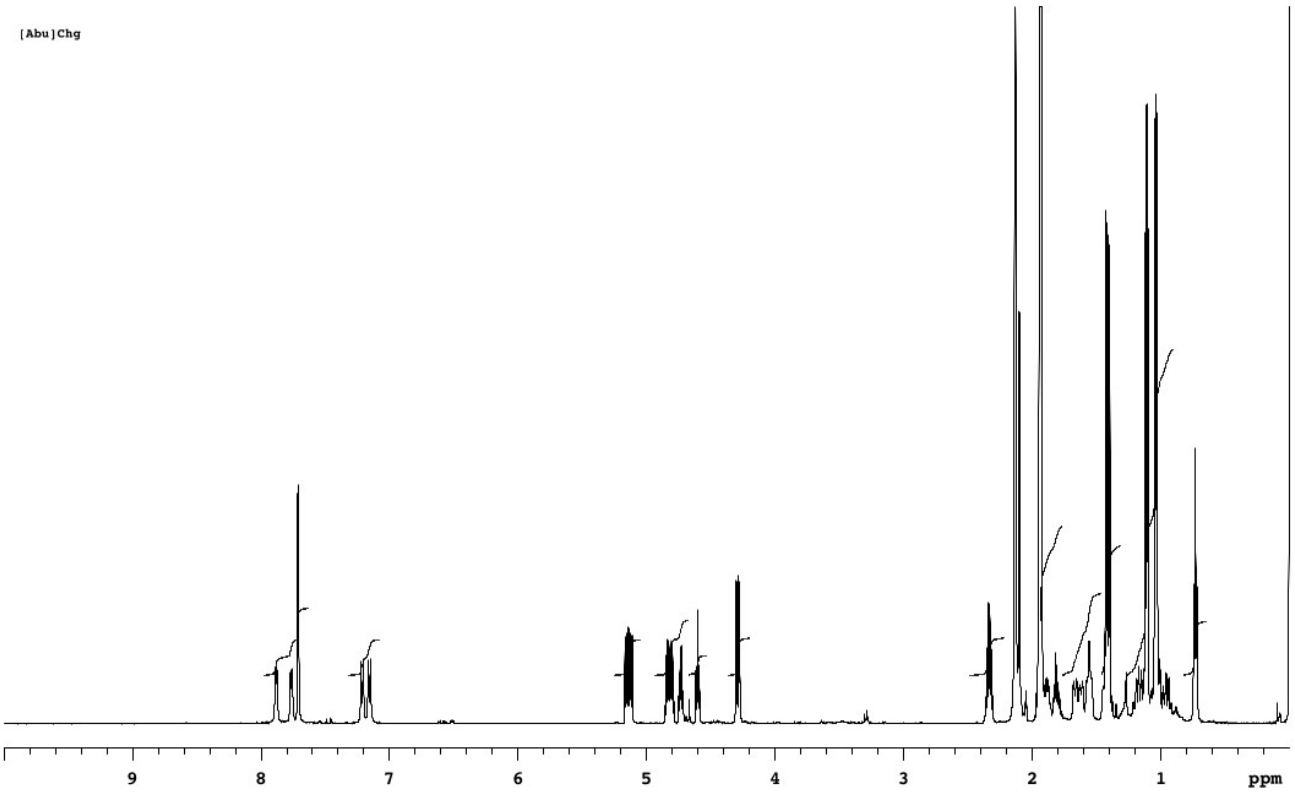

Fig. S4 1D ^{1}H NMR spectrum of peptide **3b** in CD_3CN at 298 K.

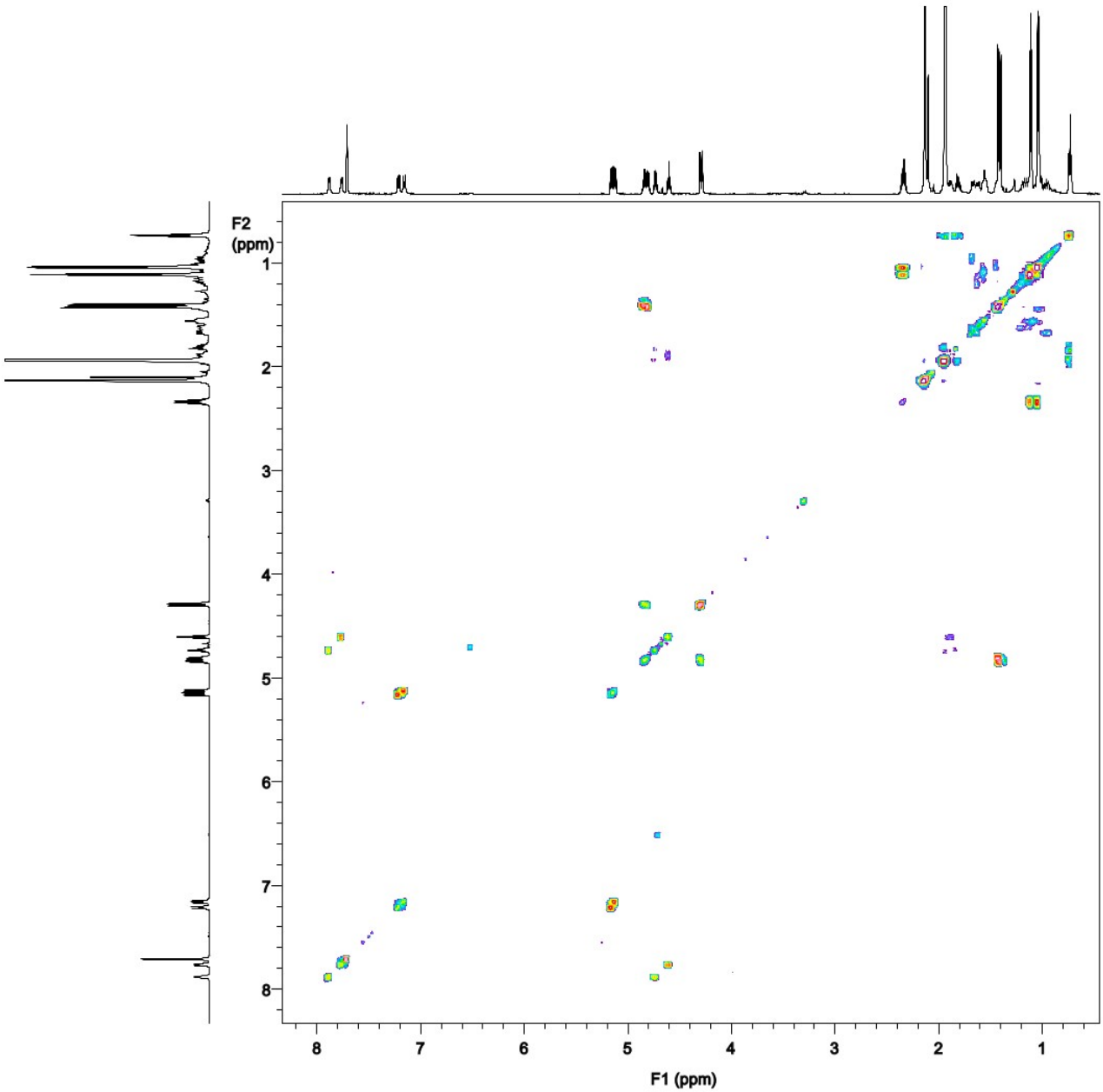

Fig. S5 2D ^{1}H-^{1}H COSY spectrum of peptide **3b** in CD_3CN at 298 K.

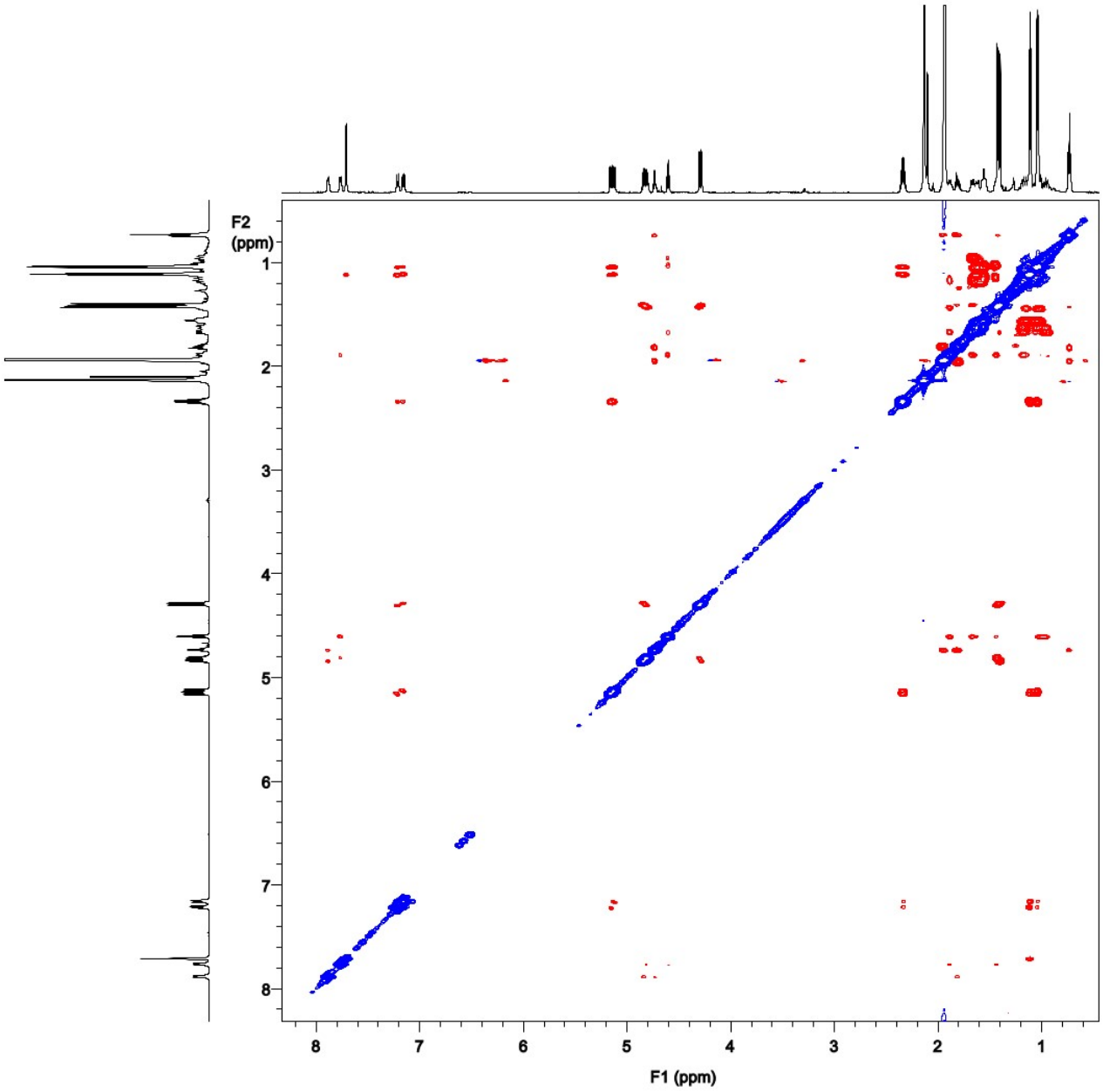

Fig. S6 2D ^{1}H-^{1}H ROESY spectrum of peptide **3b** in CD_3CN at 298 K.

^{1}H NMR spectra of peptides 4b

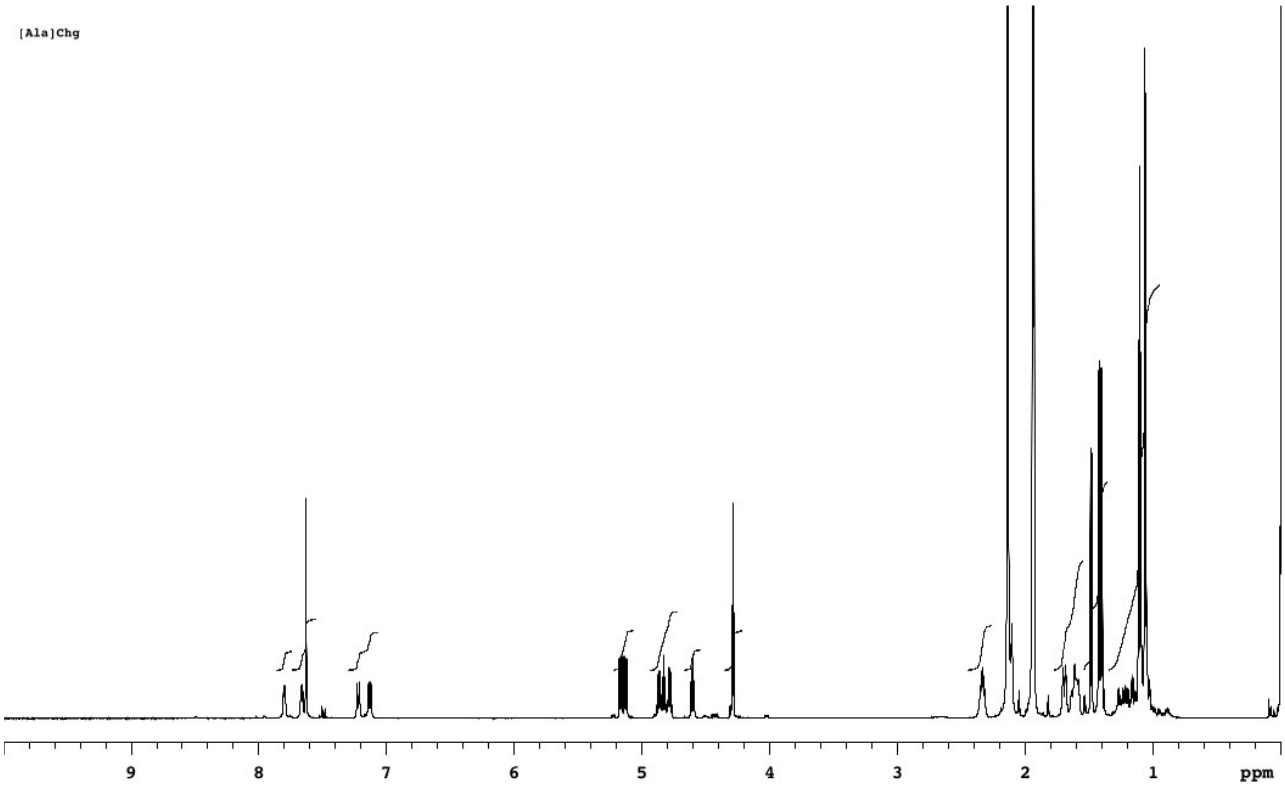

Fig. S7 1D ^{1}H NMR spectrum of peptide **4b** in CD_3CN at 298 K.

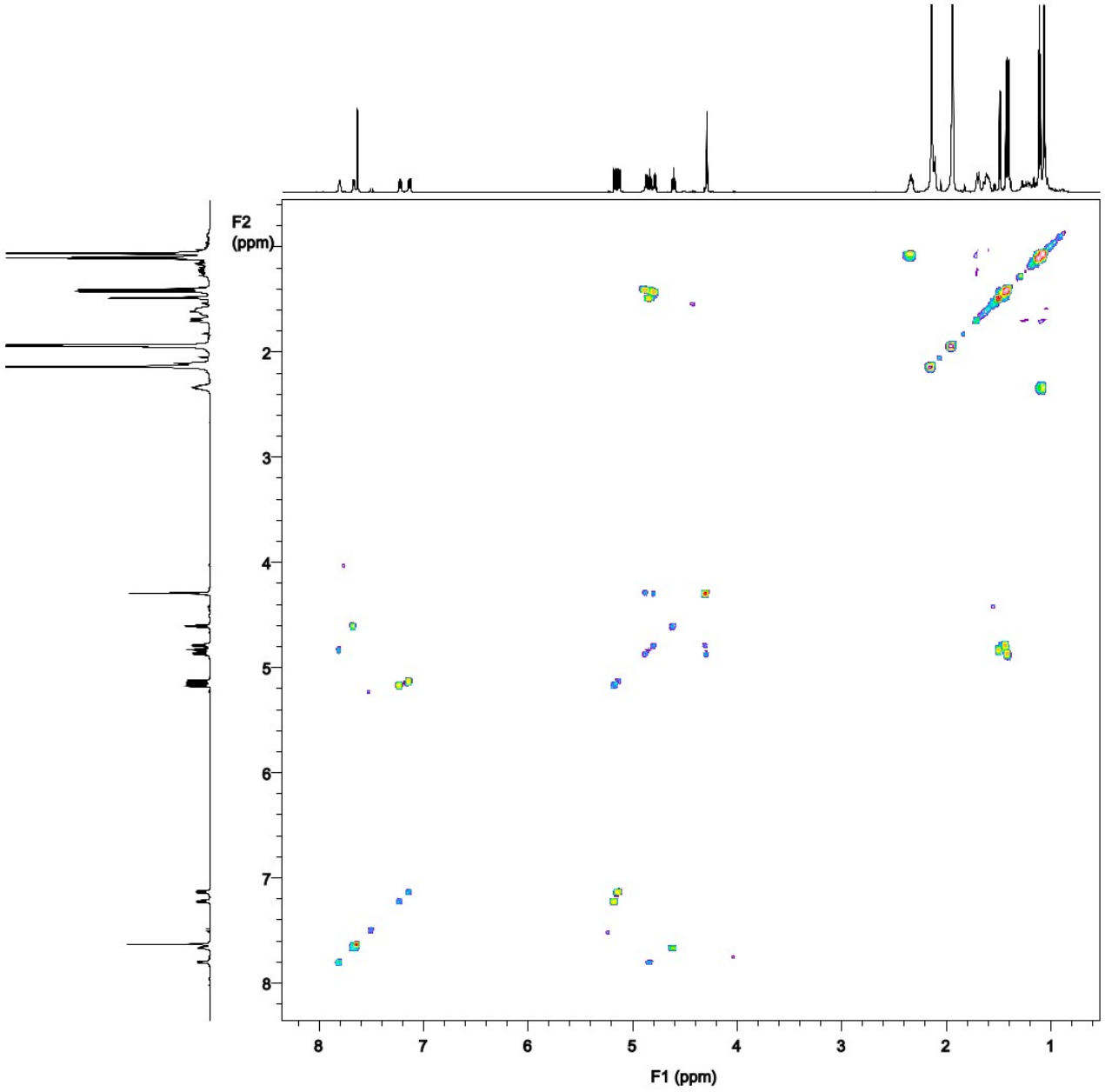

Fig. S8 2D ^{1}H-^{1}H COSY spectrum of peptide **4b** in CD_3CN at 298 K.

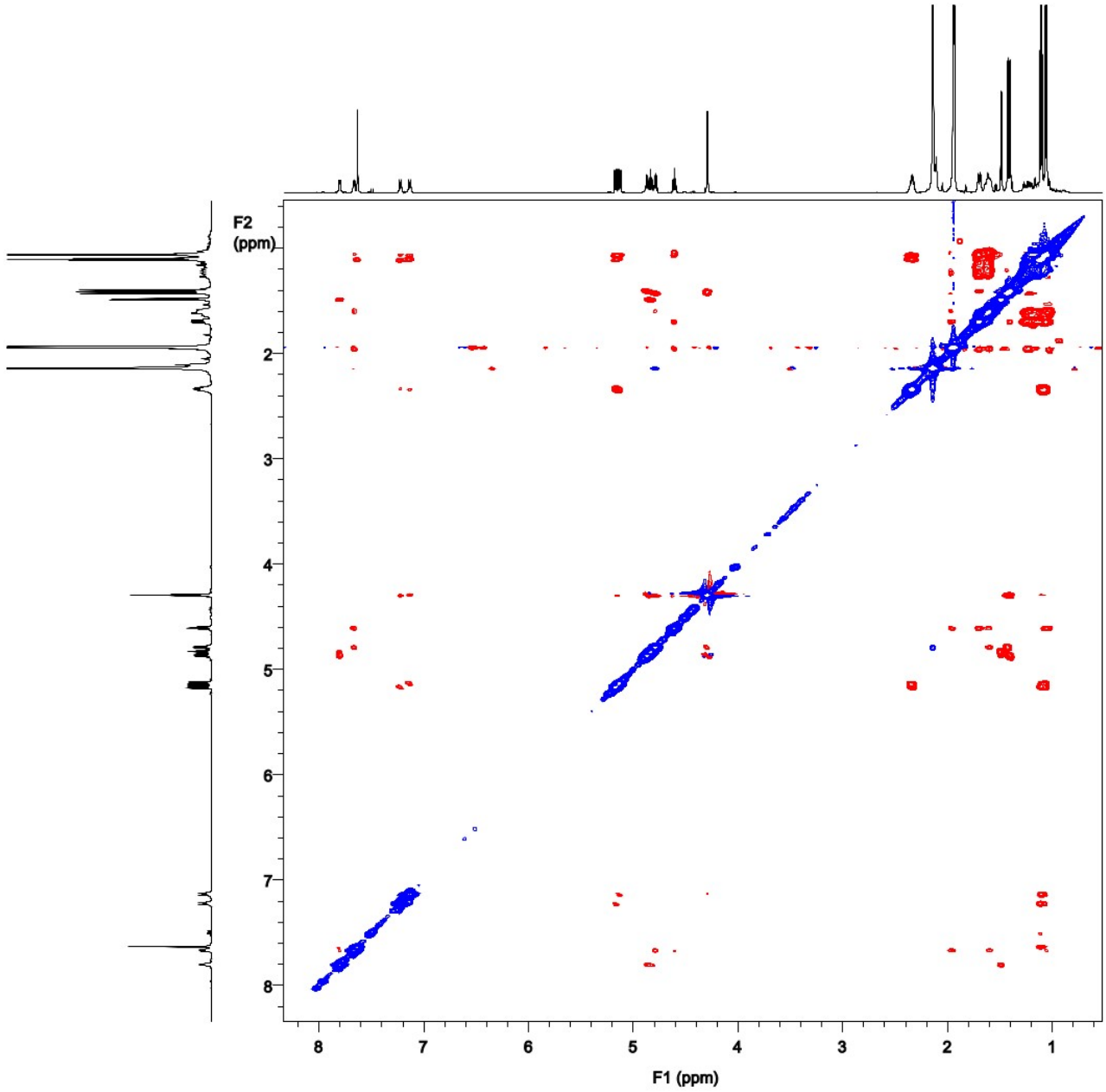

Fig. S9 2D ^{1}H-^{1}H ROESY spectrum of peptide **4b** in CD_3CN at 298 K.

^{1}H NMR spectra of peptides 2c

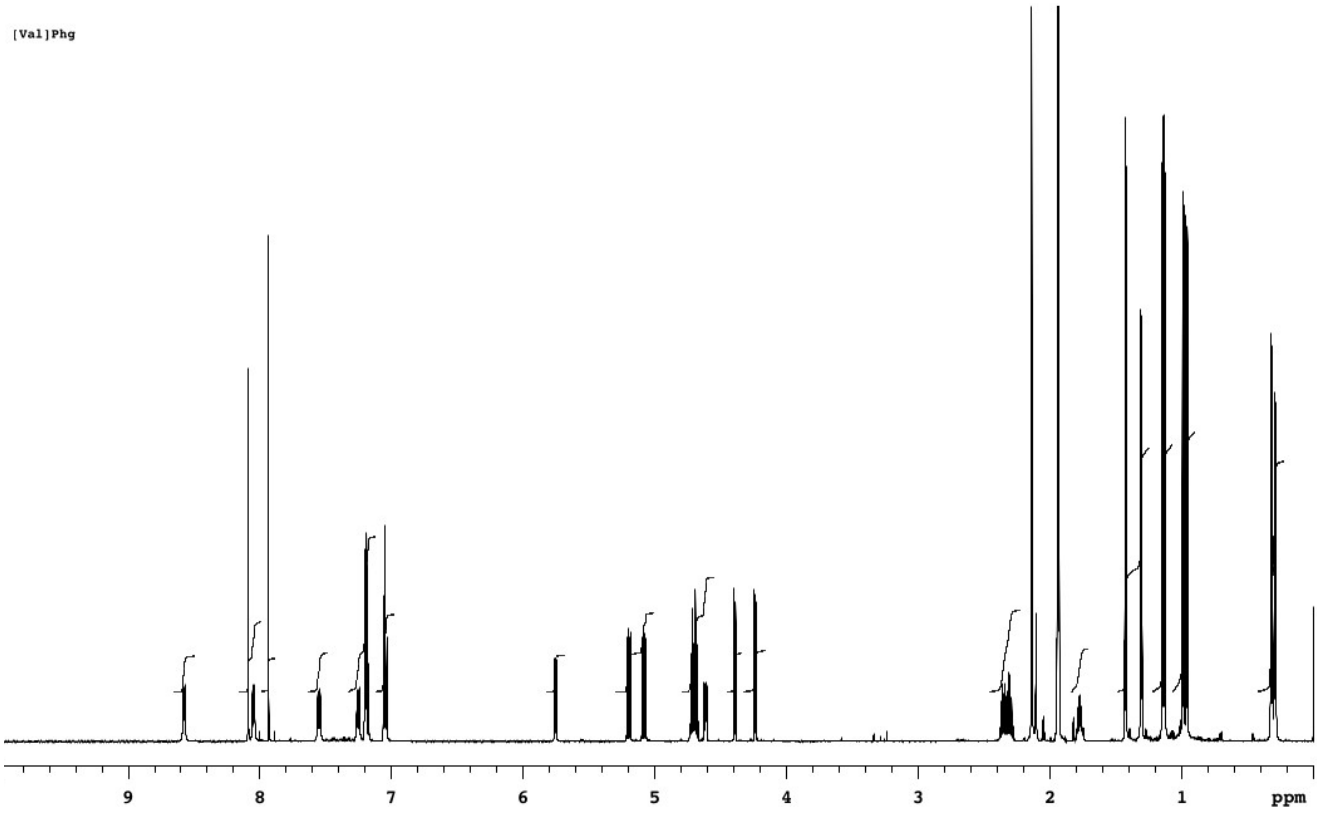

Fig. S10 1D ^{1}H NMR spectrum of peptide **2c** in CD_3CN at 298 K.

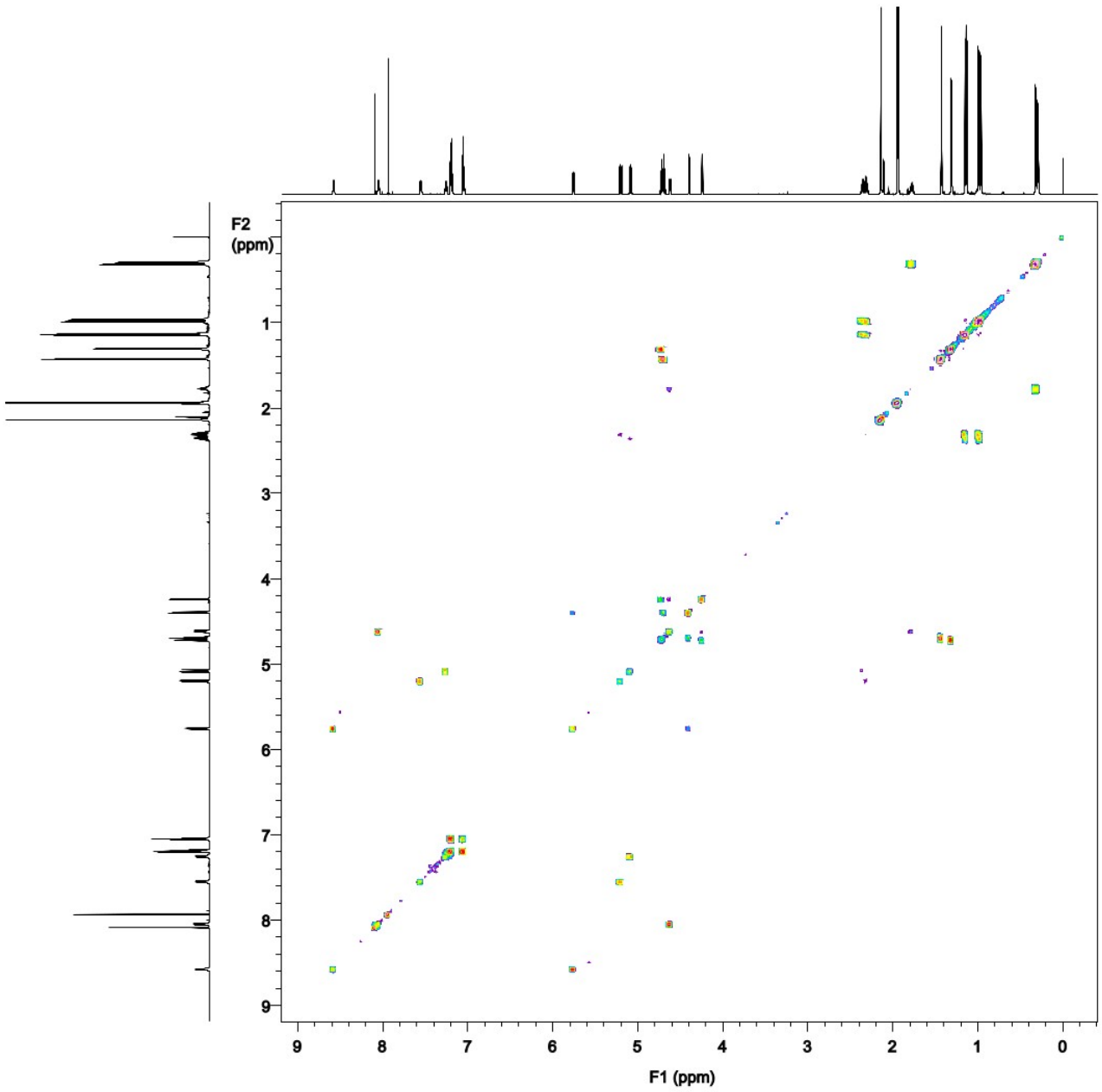

Fig. S11 2D ^{1}H-^{1}H COSY spectrum of peptide **2c** in CD_3CN at 298 K.

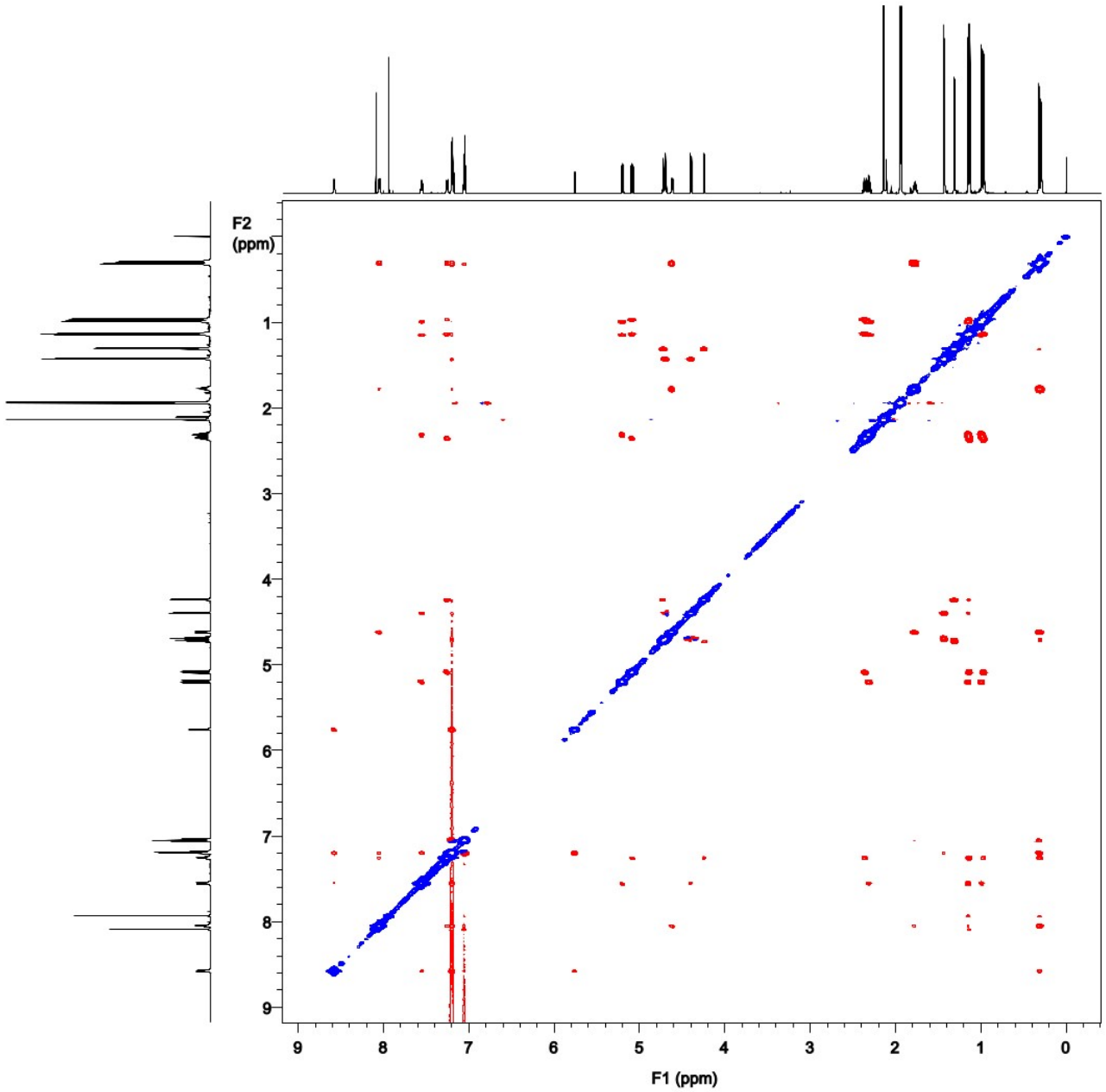

Fig. S12 2D ^{1}H-^{1}H ROESY spectrum of peptide **2c** in CD_3CN at 298 K.

^{1}H NMR spectra of peptides 3c

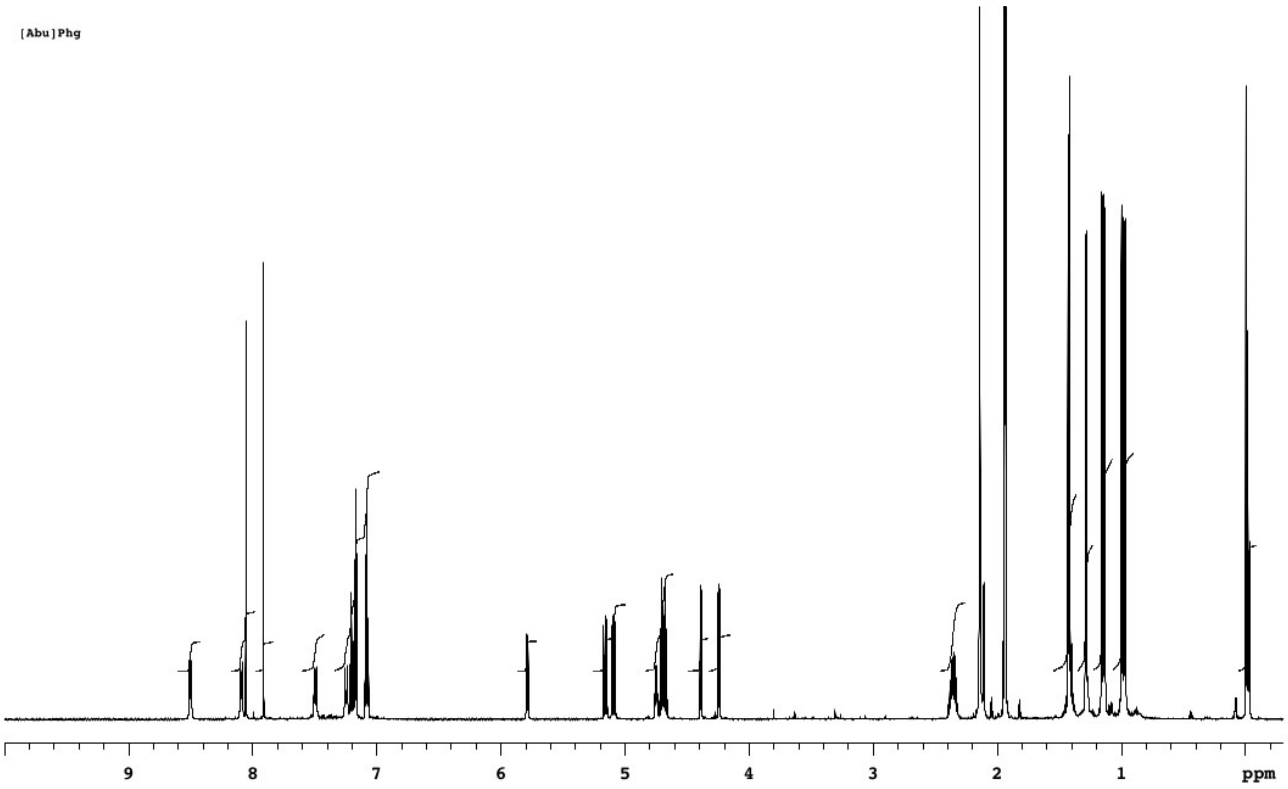

Fig. S13 1D ^{1}H NMR spectrum of peptide **3c** in CD_3CN at 298 K.

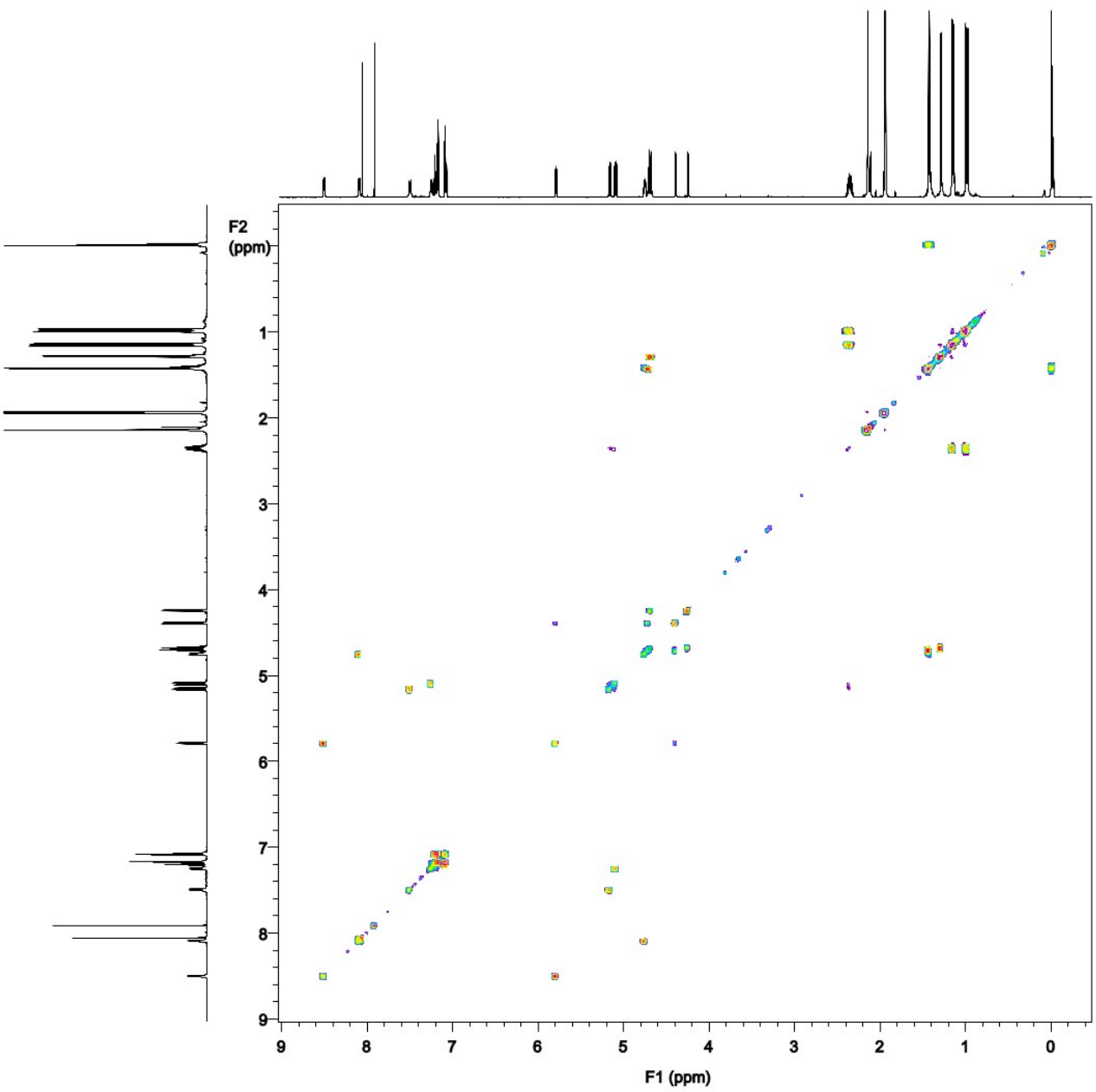

Fig. S14 2D ^{1}H-^{1}H COSY spectrum of peptide **3c** in CD_3CN at 298 K.

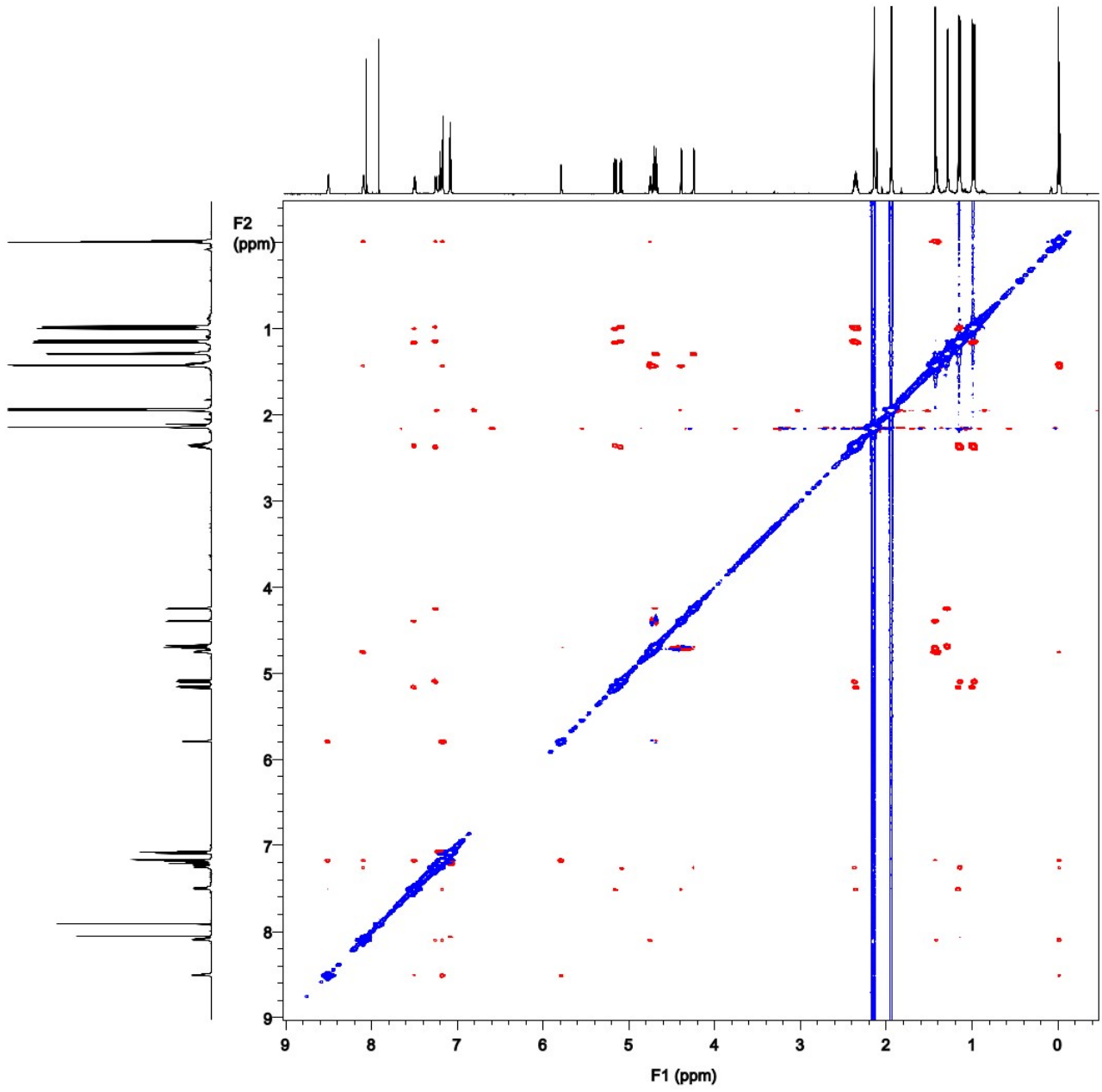

Fig. S15 2D ^{1}H-^{1}H ROESY spectrum of peptide **3c** in CD_3CN at 298 K.

^{1}H NMR spectra of peptides 4c

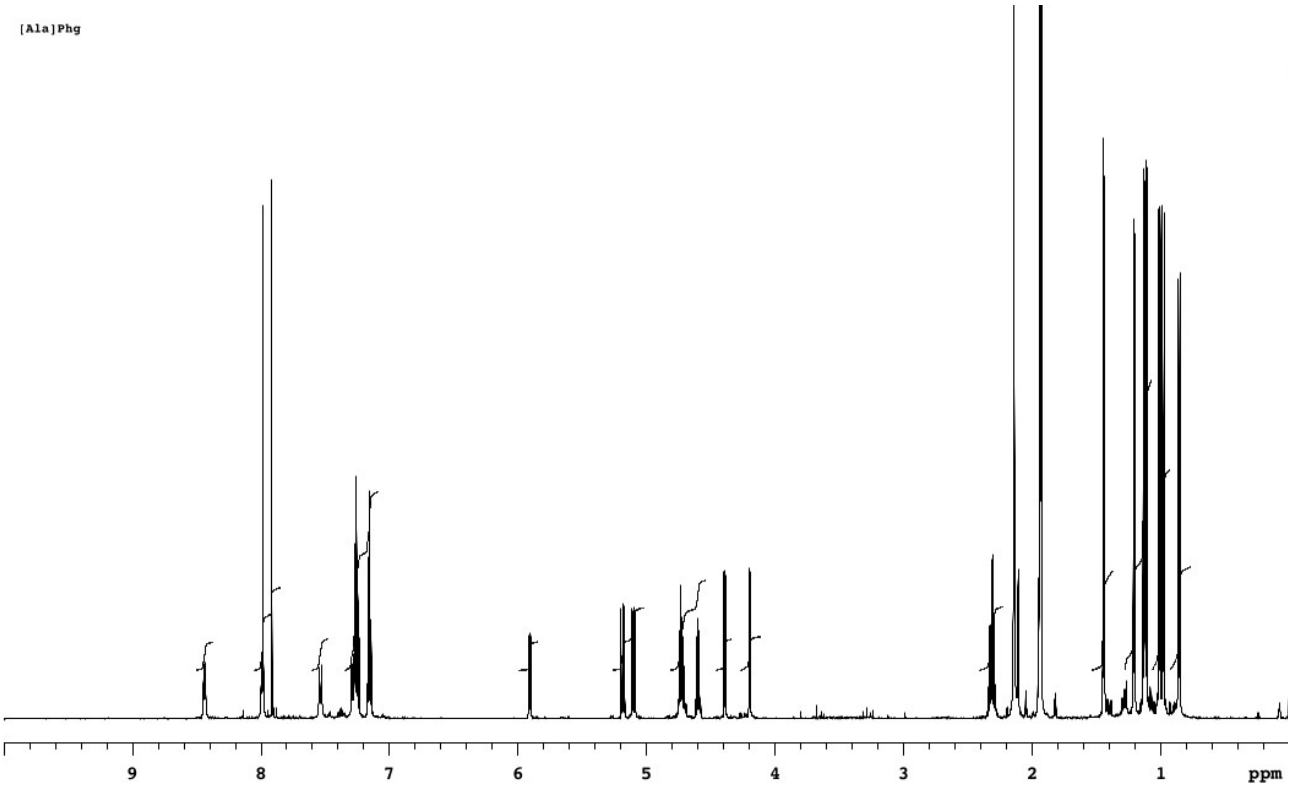

Fig. S16 1D ^{1}H NMR spectrum of peptide **4c** in CD_3CN at 298 K.

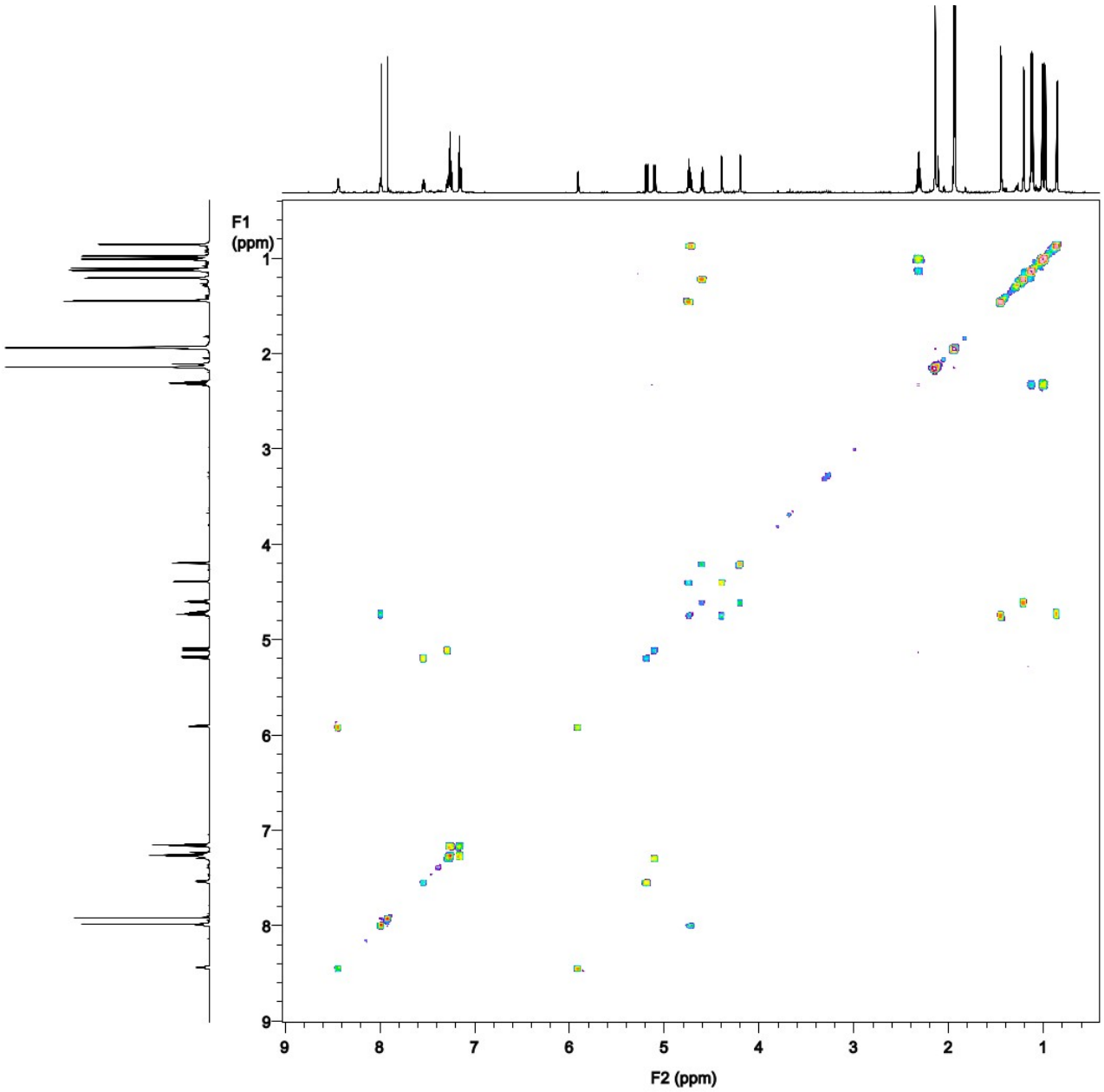

Fig. S17 2D ^{1}H-^{1}H COSY spectrum of peptide **4c** in CD_3CN at 298 K.

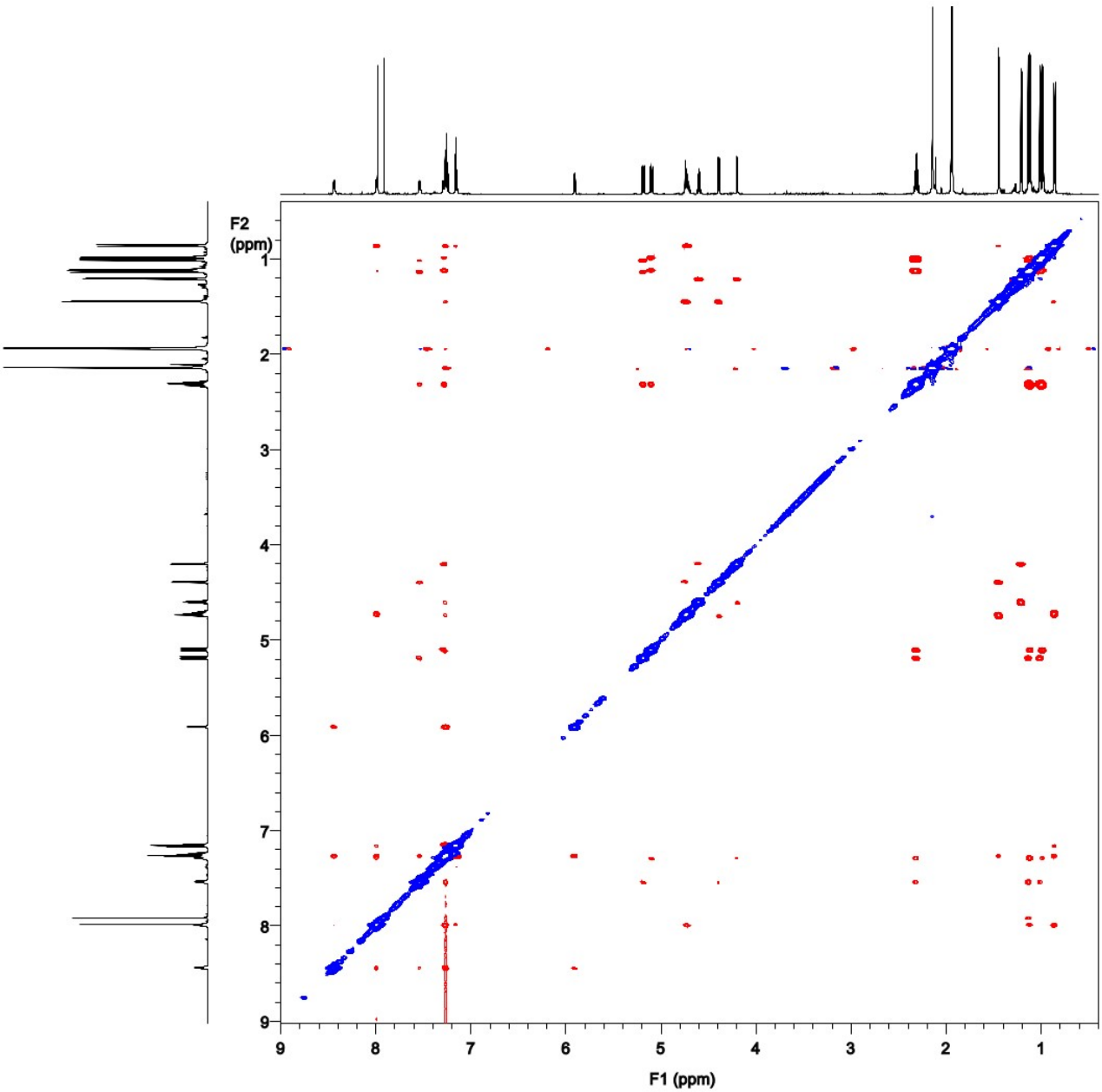

Fig. S18 2D ^{1}H-^{1}H ROESY spectrum of peptide **4c** in CD_3CN at 298 K.

Crystallographic data for peptides 2b and 2c.

Table S1. Crystal and experimental data for **2b** and **2c**.

Peptide	**2b**	**2c**
Formula	$C_{37}H_{52}N_8O_6S_2$, C_4H_9NO	$C_{38}H_{47}N_8O_6S_2$, C_4H_9NO
Formula Weight	856.11	863.08
Cell System	monoclinic	monoclinic
Space Group	$P2_1$	C2
a, Å	12.012(2)	18.269(6)
b, Å	12.909(3)	12.967(4)
c, Å	14.885(3)	11.641(4)
α, deg	90.00	90.00
β, deg	97.85(3)	123.754(4)
γ, deg	90.00	90.00
Volume, Å^3	2286.5(8)	2292.9(13)
Z	2	2
Dc, g cm^{-3}	1.243	1.250
F(000)	916	918
μ, mm^{-1}	1.518(Cu Kα)	0.173 (Mo Kα)
Wavelength, Å	1.54184	0.71073
No. of reflections (obs)	8579	3907
R_{INT}	0.0818	0.0362
θ_{max}, deg	70.07	25.02
No. of reflections (I>2σ(I))	8214	3055
Flack parameter	0.005 (18)	-0.3(3)
*R*1	0.0644	0.1071
wR	0.1733	0.2655
Goodness of fit	0.744	1.141
$(\Delta/\sigma)_{max}$	0.002	0.017
Fraction for θ_{max}	1.000	0.997
$\Delta\rho_{max}$, e Å^{-3}	0.959	0.660
$\Delta\rho_{min}$, e Å^{-3}	–0.334	–0.691
CCDC Number	2191404	2191405

The CH···π contacts within the crystal structures of 1c and 2c

The distances between the side chains of Xaa[1] and Phg[5] were estimated by surveying the CH···π contacts for the six-membered π-system, as described by Umezawa *et al*. (Y. Umezawa *et al*., *Bull*. *Chem*. *Soc*. *Jpn*., 1998, **71**, 1207-1213) (Fig. S19). The distance between a C-H hydrogen atom and the π-plane, the distance between H and the line C^1-C^2, and the H/C^1 interatomic distance are defined as D_{pln}, D_{lin} and D_{atm}, respectively. These distance parameters (D_{pln}, D_{lin} and D_{atm}) correspond to regions 1, 2 and 3, respectively. A C-H hydrogen atom is positioned above the π-plane in region 1 or at a position where it is able to contact the π-orbital in regions 2 and 3. An alkyl group can interact with the π-group in regions where the hydrogen atom is above the π-plane but slightly offset, outside the ring. The dihedral angles determined by the π-plane, plane H-C^1-C^2 and angle ∠H-X-C^1 (X=C, O, etc.) are defined as ω and θ, respectively. The distances from the H atoms of the Xaa[1] alkyl side chain to the π-orbital of the Phg[5] residue in the crystal structures of **1c** and **2c** are listed in Table 2.

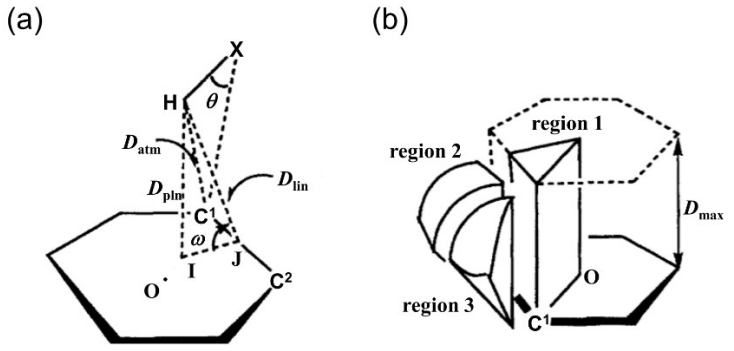

Fig. S19 Method for surveying CH···π contacts in a six-membered π-system (Y. Umezawa *et al*., *Bull*. *Chem*. *Soc*. *Jpn*., 1998, **71**, 1207-1213). (a) O: center of the plane. C^1 and C^2: nearest and second nearest sp^2-carbons to H. ω: dihedral angle defined by the C^1OC^2 and HC^1C^2 planes. θ: ∠HXC^1. D_{pln}: H/π-plane distance (H/I). D_{atm}: interatomic distance (H/C^1). D_{lin}: distance between H and line C^1C^2 (H/J). (b) 1: region where H is above the aromatic ring. 2 and 3: regions where H is outside region 1 but may interact with the π-orbitals. $D_{pln} < D_{max}$, $\theta < 60^\circ$, $|\omega| < 90^\circ$ for region 1; $D_{lin} > D_{max}$, $\theta < 60^\circ$, $90^\circ < |\omega| < 130^\circ$ for region 2; and $D_{atm} < D_{max}$, $\theta < 60^\circ$, $50^\circ < \phi < 90^\circ$ for region 3 (ϕ: HC^1I). (θ

should be smaller than 60˚ to avoid contact of atom X with C^1). D_{max}: cutoff value in every region.

Table S2. The distances from the H atoms of Xaa^1 side chains to the π-orbital of the Phg^5 residue and angle parameters (θ and ω) within the crystal structures of **1c** and **2c** were estimated by surveying the CH···π contacts in a six-membered π-system.

	1c[a] (Ile^1)			**2c** (Val^1)	
	βH	γ^2H	δH	βH	γ^1H
θ (˚)	33.8	21.3	59.0	34.8	33.6
ω (˚)	115.6	108.7	89.2	119.7	129.2
Region	2	2	1	2	2
Distance (Å)	3.71[b]	3.17[b]	4.52[c]	4.00[b]	3.75[b]

[a] These parameters for **1c** are estimated from a previously reported crystal structure (A. Asano *et al*., *Bioorg. Med. Chem*., 2011, **19**, 3372–3377).

[b] These distance parameters determined as D_{lin} correspond to region 2.

[c] This distance parameter determined as D_{pln} corresponds to region 1.

Temperature coefficients of protons of Xaa[1] alkyl side chain in Xc peptides.

Table S3. Temperature dependences of chemical shifts for alkyl protons of Ile[1] side chain of **1c**.

T (K)	δ Ile[1] βH (ppm)	δ Ile[1] γ^{11}H (ppm)	δ Ile[1] γ^{12}H (ppm)	δ Ile[1] γ^{2}H (ppm)	δ Ile[1] δH (ppm)
273	ND	0.963	0.664	0.120	0.346
283	ND	0.960	0.664	0.145	0.355
293	ND	0.972	0.672	0.167	0.365
303	1.457	0.984	0.682	0.189	0.376
313	1.474	0.981	0.692	0.209	0.387
323	1.487	1.009	0.710	0.228	0.399
333	1.508	1.022	0.717	0.246	0.412
Δδ/ΔT (ppb/K)	1.7	1.1	1.0	2.1	1.1

Table S4. Temperature dependences of chemical shifts for alkyl protons of Val[1] side chain of **2c**.

T (K)	δ Val[1] βH (ppm)	δ Val[1] γ^{1}H(ppm)	δ Val[1] γ^{2}H (ppm)
273	1.747	0.288	0.260
283	1.759	0.301	0.274
293	1.771	0.314	0.287
303	1.782	0.327	0.300
313	1.792	0.338	0.314
323	1.802	0.350	0.329
333	1.812	0.362	0.344
Δδ/ΔT (ppb/K)	1.1	1.2	1.4

Table S5. Temperature dependences of chemical shifts for alkyl protons of Abu[1] side chain of **3c**.

T (K)	δ Abu[1] βH (ppm)	δ Abu[1] γH (ppm)
273	1.394	-0.067
283	1.404	-0.047
293	1.413	-0.029
303	1.422	-0.009
313	1.432	0.010
323	1.440	0.030
333	1.448	0.051
Δδ/ΔT (ppb/K)	0.9	2.0

Table S6. Temperature dependences of chemical shifts for alkyl protons of Ala[1] side chain of **4c**.

T (K)	δ Ala^{1} βH (ppm)
273	0.839
283	0.848
293	0.855
303	0.862
313	0.869
323	0.877
333	0.886
$\Delta\delta/\Delta$T (ppb/K)	0.8

Thermodynamic parameters and van't Hoff plots for peptides Xb and Xc (X=2-4).

Table S7. Equilibrium parameters of peptide **2b**.

T (K)	Thz H (ppm)	*K**	ΔG^0 (J•mol^{-1})**
273	7.67	1.284	-567
283	7.70	1.090	-204
293	7.74	0.902	250
303	7.77	0.764	678
313	7.80	0.652	1114
323	7.82	0.560	1559
333	7.85	0.484	2006

*Equilibrium constants were calculated from the average value of the chemical shifts of Thz^4 and Thz^8 protons: $K = (\delta_s - \delta_{obs}) / (\delta_{obs} - \delta_f)$. δ_s (8.09 ppm) is the chemical shift for Thz proton of T3ASC. δ_f (7.35 ppm) is the chemical shift for Thz proton of *d*ASC at 273 K.

**$\Delta G^o = -RT\ln K$

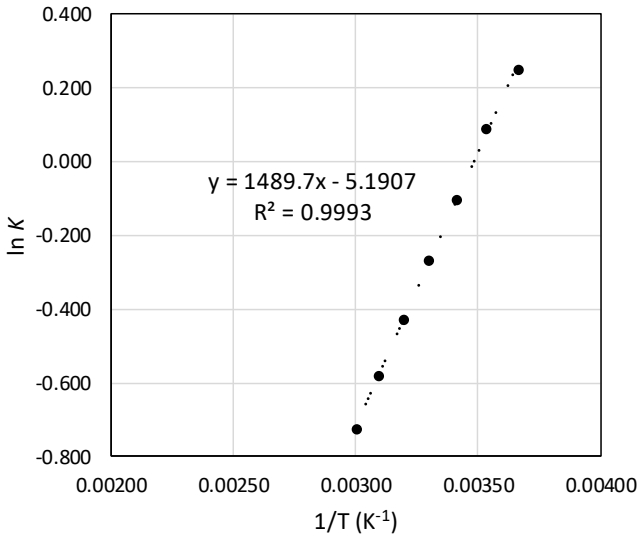

Fig. S20 van't Hoff plot of peptide **2b**.

Table S8. Thermodynamic parameters of peptide **2b**.

ΔH^0 (kJ•mol^{-1})	ΔS^0 (J•mol^{-1})	ΔG^0_{298K} (kJ•mol^{-1})*
-12.39	-43.16	0.47

*$\Delta G^o = \Delta H^o - T\Delta S^o$

Table S9. Equilibrium parameters of peptide **3b**.

T (K)	Thz H (ppm)	*K**	ΔG^0 (J•mol^{-1})**
273	7.64	1.561	-1010
283	7.67	1.316	-646
293	7.70	1.123	-283
303	7.73	0.960	102
313	7.76	0.820	515
323	7.78	0.707	931
333	7.81	0.612	1359

*Equilibrium constants were calculated from the average value of the chemical shifts of Thz^4 and Thz^8 protons: $K = (\delta_s - \delta_{obs}) / (\delta_{obs} - \delta_f)$. δ_s (8.09 ppm) is the chemical shift for Thz proton of T3ASC. δ_f (7.35 ppm) is the chemical shift for Thz proton of *d*ASC at 273 K.

**$\Delta G^o = - RT\ln K$

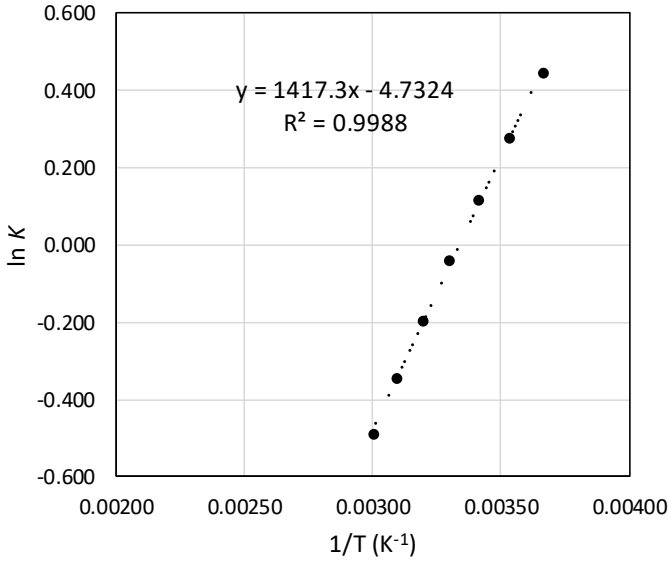

Fig. S21 van't Hoff plot of peptide **3b**.

Table S10. Thermodynamic parameters of peptide **3b**.

ΔH^0 (kJ•mol^{-1})	ΔS^0 (J•mol^{-1})	ΔG^0_{298K} (kJ•mol^{-1})*
-11.78	-39.35	-0.06

*$\Delta G^o = \Delta H^o - T\Delta S^o$

Table S11. Equilibrium parameters of peptide **4b**.

T (K)	Thz^{4or8} H (ppm)	*K**	ΔG^0 (J•mol^{-1})**
273	7.55	2.795	-2333
283	7.58	2.217	-1874
293	7.62	1.782	-1407
298	7.63	1.624	-1202
303	7.65	1.442	-923
313	7.69	1.173	-416
323	7.73	0.968	87
333	7.76	0.805	601

*Equilibrium constants were calculated from the average value of the chemical shifts of Thz^4 and Thz^8 protons: $K = (\delta_s - \delta_{obs}) / (\delta_{obs} - \delta_f)$. δ_s (8.09 ppm) is the chemical shift for Thz proton of T3ASC. δ_f (7.35 ppm) is the chemical shift for Thz proton of *d*ASC at 273 K.

**$\Delta G^o = - RT\ln K$

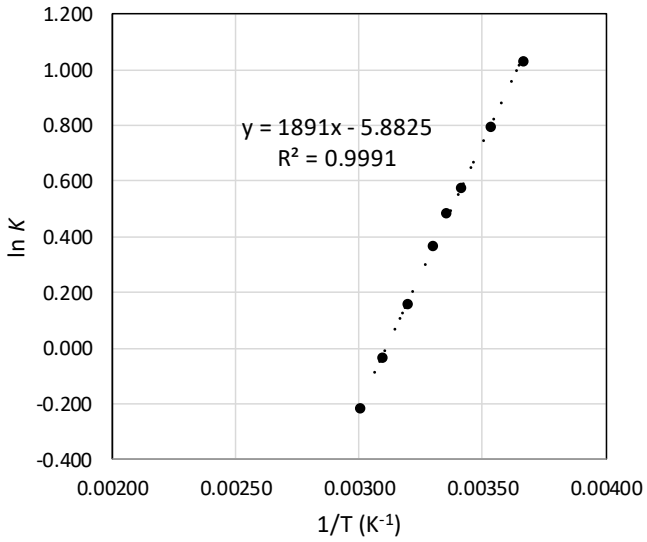

Fig. S22 van't Hoff plot of peptide **4b**.

Table S12. Thermodynamic parameters of peptide **4b**.

ΔH^0 (kJ•mol^{-1})	ΔS^0 (J•mol^{-1})	ΔG^0_{298K} (kJ•mol^{-1})*
-15.72	-48.91	-1.15

*$\Delta G^o = \Delta H^o - T\Delta S^o$

Table S13. Equilibrium parameters of peptide **2c**.

T (K)	Thz H (ppm)	*K**	ΔG^0 (J•mol^{-1})**
273	8.00	0.137	4516
283	8.01	0.128	4836
293	8.01	0.120	5175
303	8.02	0.111	5535
313	8.02	0.104	5899
323	8.03	0.096	6285
333	8.03	0.089	6696

*Equilibrium constants were calculated from the average value of the chemical shifts of Thz^4 and Thz^8 protons: $K = (\delta_s - \delta_{obs}) / (\delta_{obs} - \delta_f)$. δ_s (8.09 ppm) is the chemical shift for Thz proton of T3ASC. δ_f (7.35 ppm) is the chemical shift for Thz proton of *d*ASC at 273 K.

**$\Delta G^o = -RT\ln K$

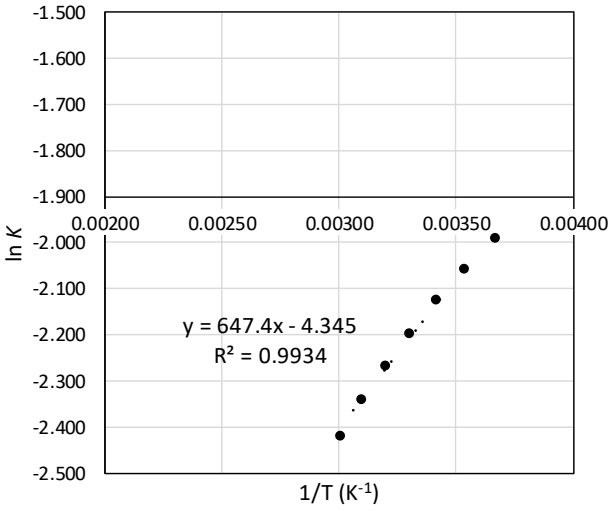

Fig. S23 van't Hoff plot of peptide **2c**.

Table S14. Thermodynamic parameters of peptide **2c**.

ΔH^0 (kJ•mol^{-1})	ΔS^0 (J•mol^{-1})	ΔG^0_{298K} (kJ•mol^{-1})*
-5.38	-36.12	5.38

*$\Delta G^o = \Delta H^o - T\Delta S^o$

Table S15. Equilibrium parameters of peptide **3c**.

T (K)	Thz H (ppm)	*K**	ΔG^0 (J•mol^{-1})**
273	7.97	0.189	3784
283	7.98	0.177	4069
293	7.99	0.165	4384
303	7.99	0.154	4720
313	8.00	0.141	5096
323	8.01	0.130	5484
333	8.01	0.120	5881

*Equilibrium constants were calculated from the average value of the chemical shifts of Thz^4 and Thz^8 protons: $K = (\delta_s - \delta_{obs}) / (\delta_{obs} - \delta_f)$. δ_s (8.09 ppm) is the chemical shift for Thz proton of T3ASC. δ_f (7.35 ppm) is the chemical shift for Thz proton of *d*ASC at 273 K.

**$\Delta G^o = -RT\ln K$

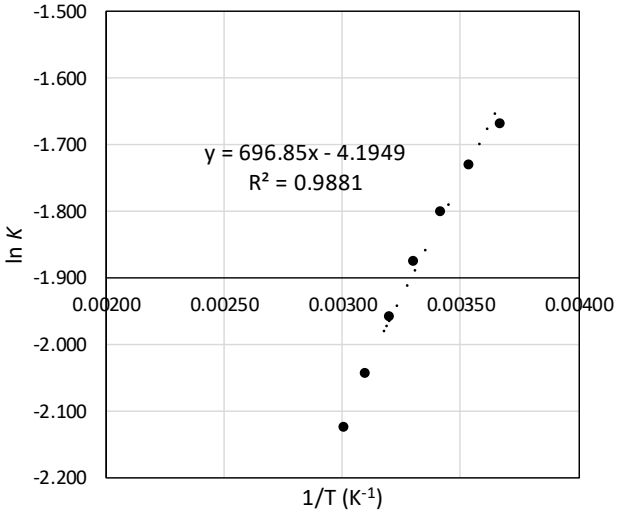

Fig. S24 van't Hoff plot of peptide **3c**.

Table S16. Thermodynamic parameters of peptide **3c**.

ΔH^0 (kJ•mol^{-1})	ΔS^0 (J•mol^{-1})	ΔG^0_{298K} (kJ•mol^{-1})*
-5.79	-34.88	4.60

*$\Delta G^o = \Delta H^o - T\Delta S^o$

Table S17. Equilibrium parameters of peptide **4c**.

T (K)	Thz^{4or8} H (ppm)	K*	ΔG^0 (J•mol^{-1})**
273	7.91	0.317	2610
283	7.93	0.278	3011
293	7.95	0.244	3439
298	7.95	0.232	3617
303	7.96	0.212	3906
313	7.98	0.184	4405
323	7.99	0.158	4954
333	8.00	0.138	5491

*Equilibrium constants were calculated from the average value of the chemical shifts of Thz^4 and Thz^8 protons: $K = (\delta_s - \delta_{obs}) / (\delta_{obs} - \delta_f)$. δ_s (8.09 ppm) is the chemical shift for Thz proton of T3ASC. δ_f (7.35 ppm) is the chemical shift for Thz proton of *d*ASC at 273 K.

**$\Delta G^o = -RT\ln K$

Fig. S25 van't Hoff plot of peptide **4c**.

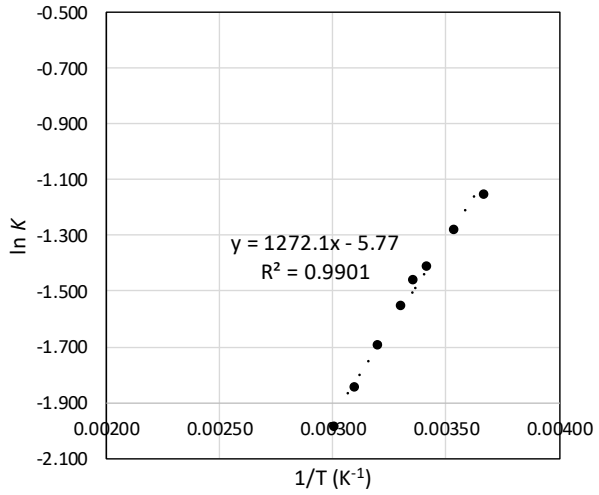

Table S18. Thermodynamic parameters of peptide **4c**.

ΔH^0 (kJ•mol^{-1})	ΔS^0 (J•mol^{-1})	ΔG^0_{298K} (kJ•mol^{-1})*
-10.58	-47.97	3.72

*$\Delta G^o = \Delta H^o - T\Delta S^o$

Cytotoxicities of peptides toward HL-60 cell.

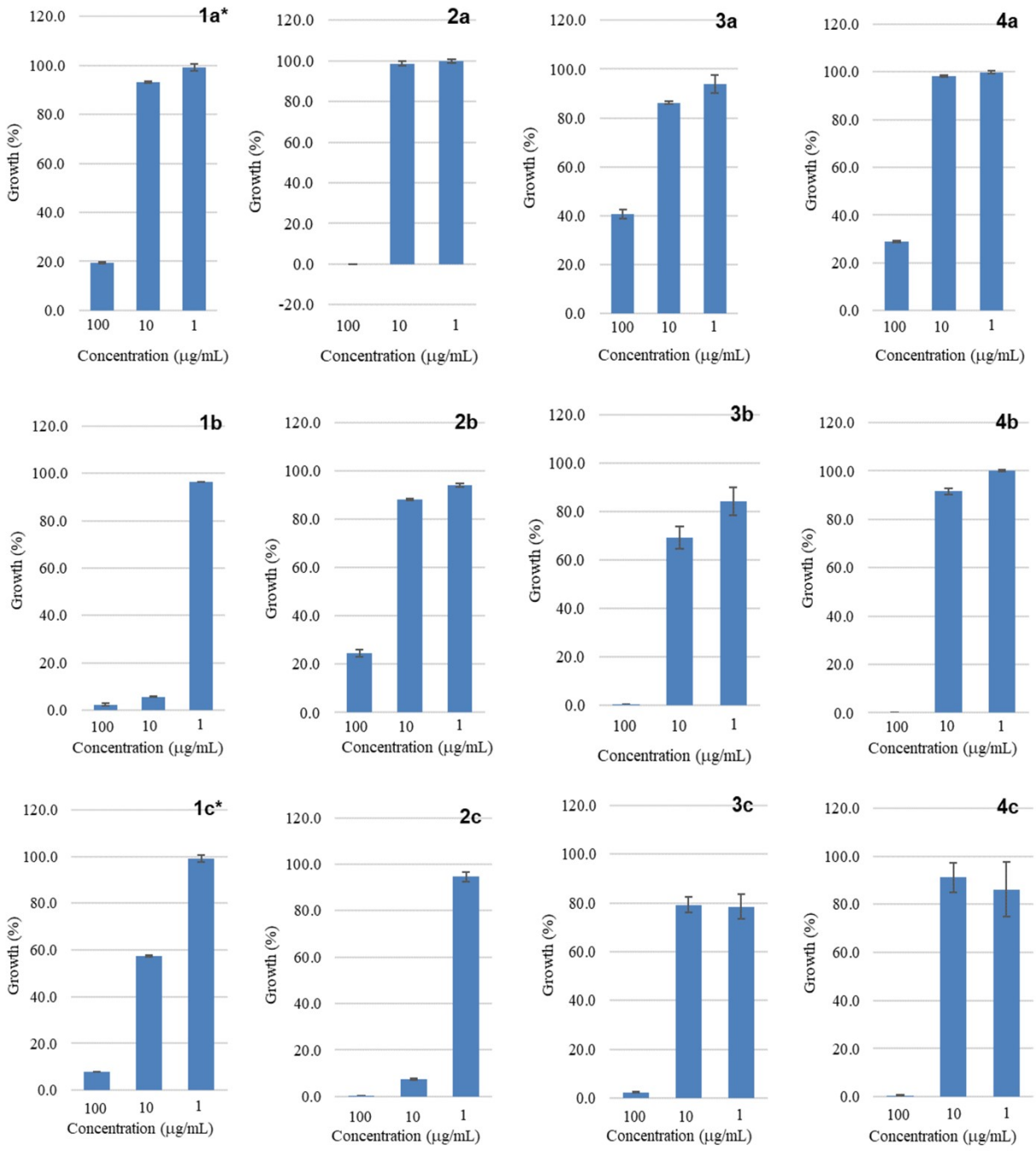

Fig. S26 Bar graph representation of cell growth data with different peptide concentration.
*These data are taken from a previous report (A. Asano *et al*., *Bioorg. Med. Chem*., 2011,**19**, 3372–3377).

Chemical structures of *d*ASC and T3ASC as reference peptides.

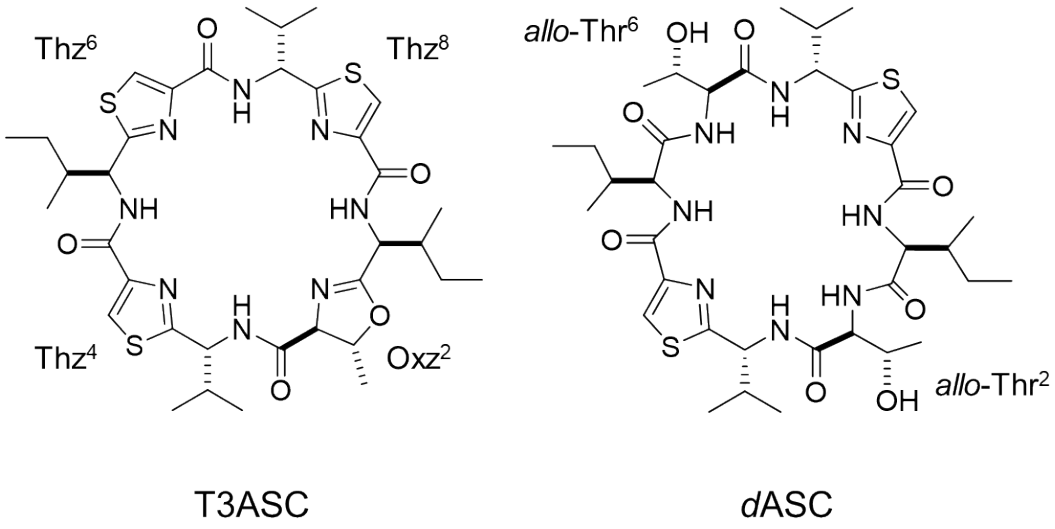

Fig. S27 Chemical structures of T3ASC (A. Asano *et al*., *J. Pept. Sci*., 2018, e3120) and *d*ASC (A. Asano *et al*., *Biopolymers*, 2001, **58**, 295–304). T3ASC and *d*ASC were used as reference peptides to provide reference chemical shifts for the fully square and folded forms, respectively.